CALIFORNIA INSTITUTE OF TECHNOLOGY

universitätbonn

Multiscale modeling of hydraulic fracture

M. Ortiz

California Institute of Technology

Rheinische Friedrich-Wilhelms Universität Bonn

SFB 1313 Seminar, Institute for Modelling Hydraulic and Environmental Systems (IWS)
University of Stuttgart, December 8, 2020

Team and sponsors

A. Pandolfi

G. della Vecchia

M.L. de Bellis

M. Ortiz

POLITECNICO MILANO 1863

UNIVERSITÀ DEL SALENTO

Caltech

Eni

Caltech NSF/IUCRC on Geomechanics and Mitigation of Geohazards

NSF

Apache

Hydraulic Fracture

- Current interest: Rock fracture by hydraulic stimulation (*fracking*) in oil/gas reservoirs to increase the reservoir production (*cheap and plentiful energy, low emissions*)

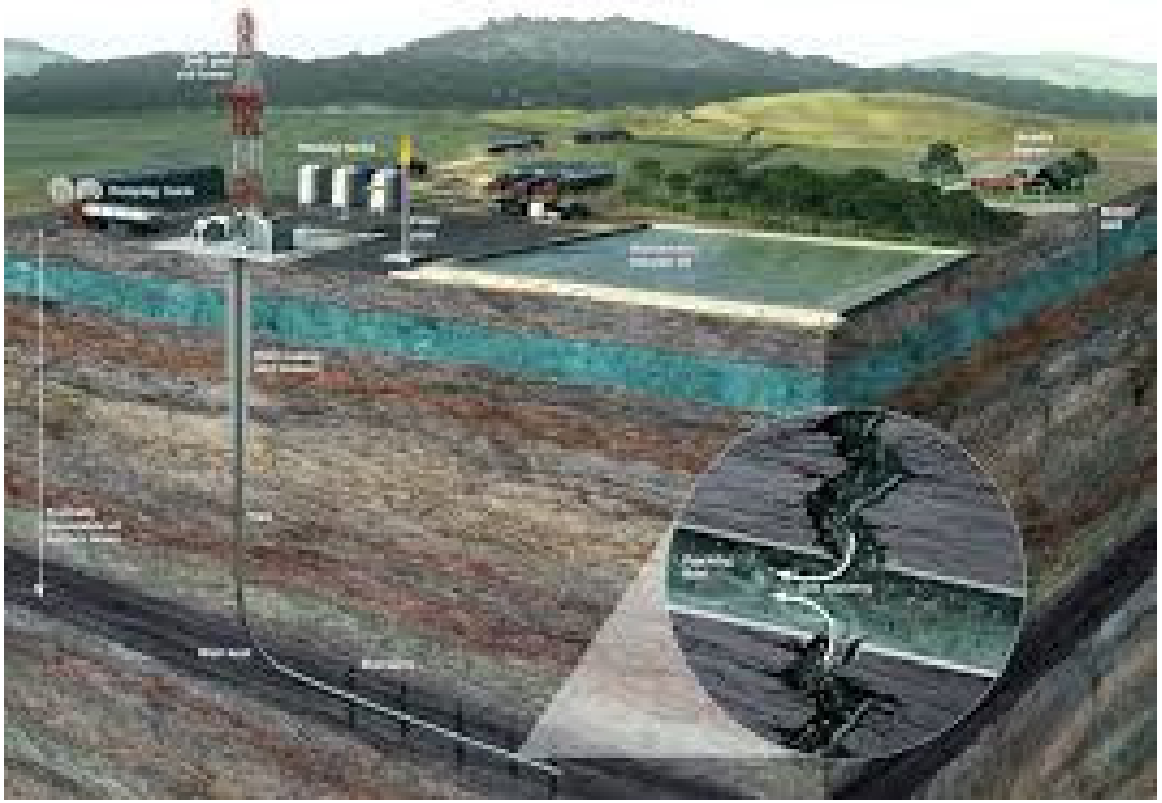

Michael Ortiz
IWS 12/08/20

Hydraulic Fracture

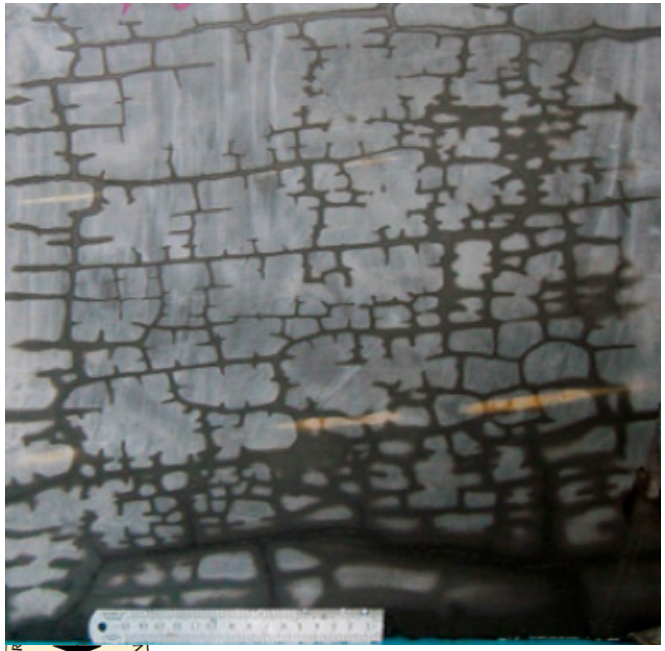

Fractures and discontinuities (faults) in natural rocks can evolve in time due to gravity, geostatic/shear stresses

Damage induced by *hydraulic stimulation* in oil/gas reservoirs can increase the reservoir production

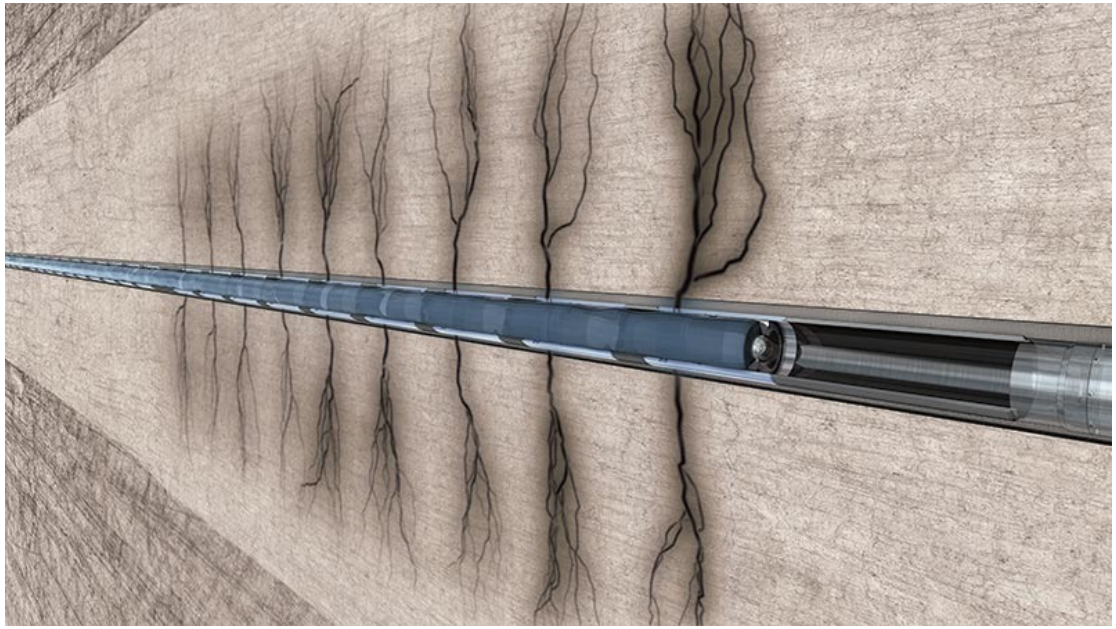

Michael Ortiz
IWS 12/08/20

Hydraulic Fracture – Complexity

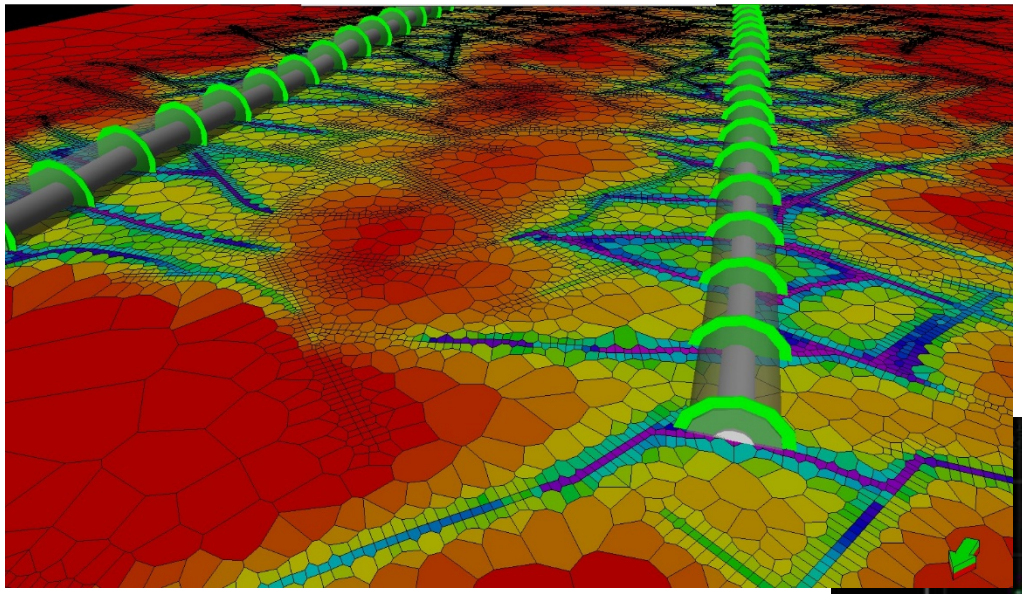

Acoustic measurements show that HF is a complex phenomenon involving the formation of intricate fracture patterns [Chuprakov *et al*., 2013, Wu *et al*., 2012]

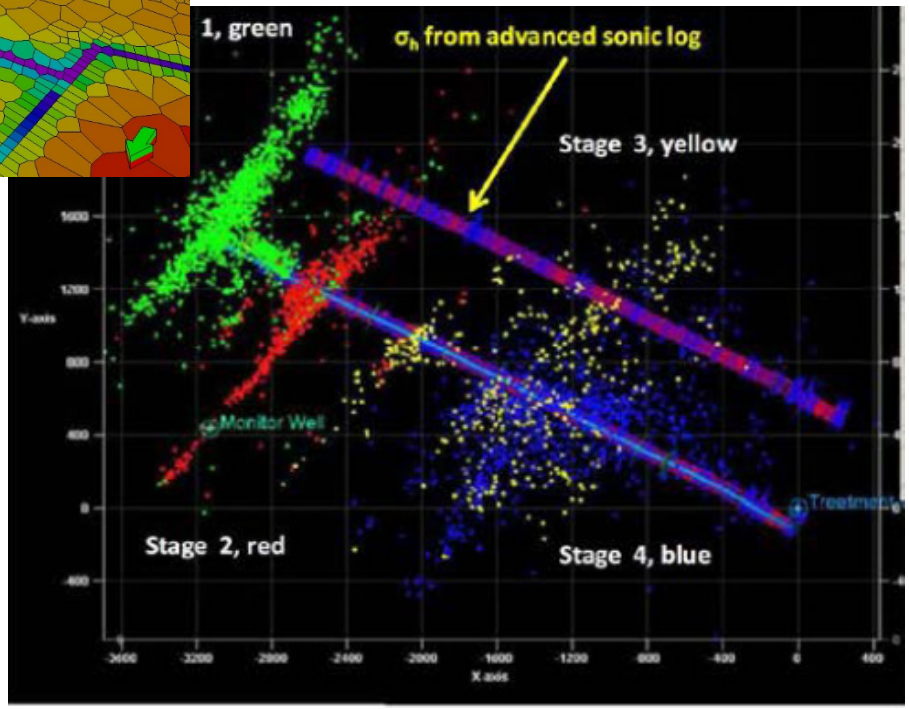

Present-day HF simulations are based on old technology. Fractures are modeled as mathematically sharp cracks, fluid flow is assumed Couette (Courtesy of Schlumberger)

Hydraulic Fracture – Multiscale

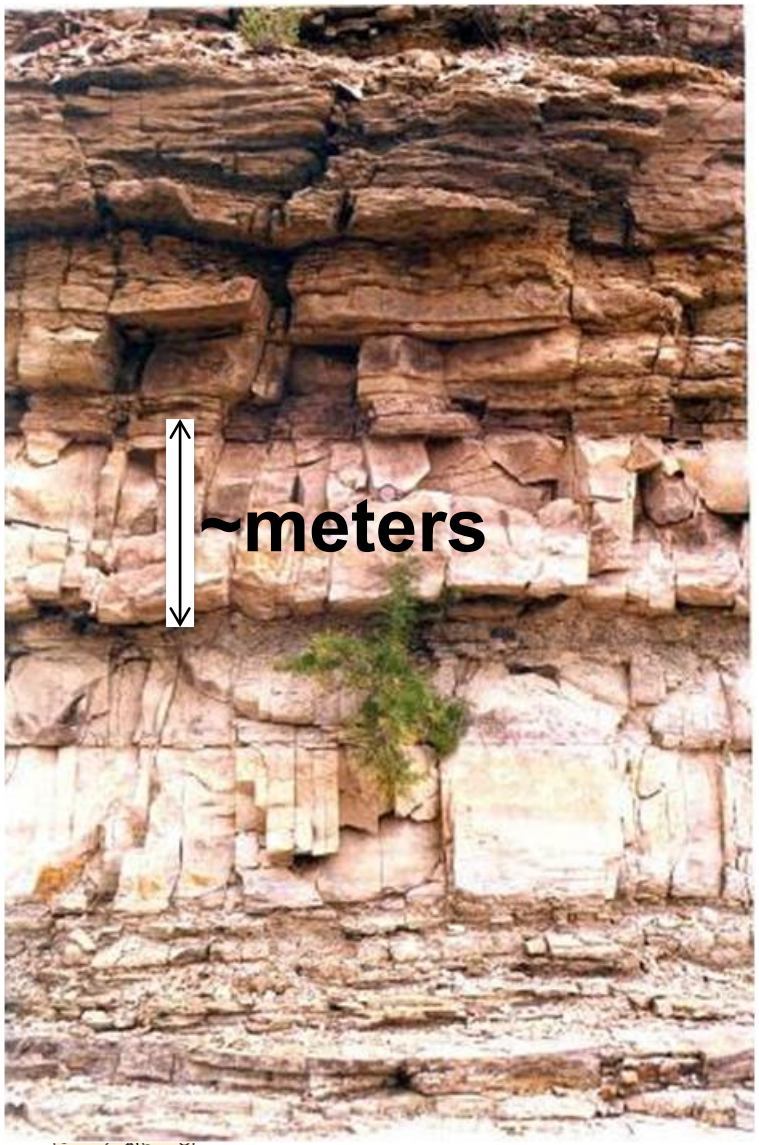

Subgrid length scales!

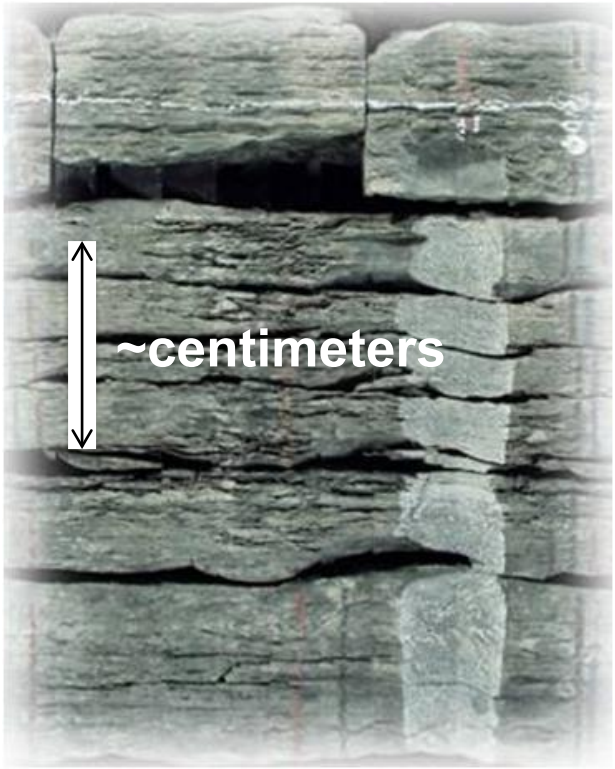

permeability

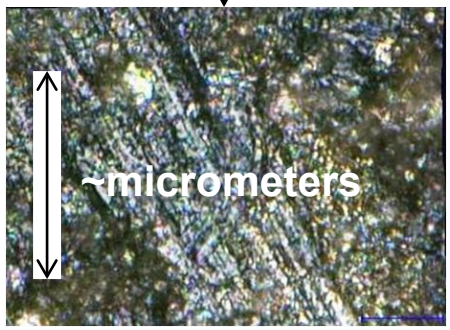

← complex multiscale rock formations

S. Green, R. Suarez-Rivera
Schlumberger Innovation Center
AAPG Geoscience Technology Workshop
July 16, 2013

Hydraulic Fracture – Fundamentals

- Rocks in compression fail through *complex fracture patterns*
- Length scales range from *microscopic to geological*
- Behavior of fracture system depends on behavior at *both micro and macroscales*:
  - *Overall geometry of HF governed by macroscopic (FE) stress analysis*
  - *Permeability governed by fine detail of microstructure* (at each FE material point)
- *Multiscale modeling!*

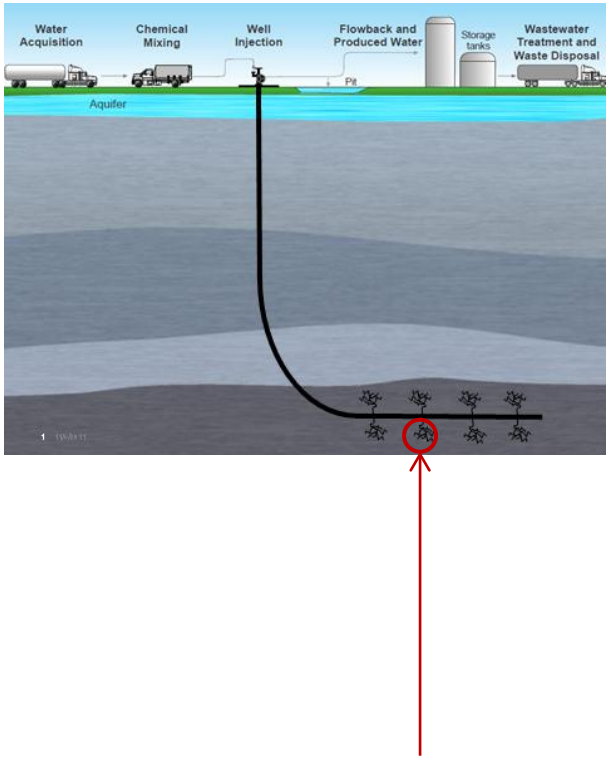

(R. Wu *et al.*, SPE-152052-MS, 2012)

How do rocks relax their stresses?

- *Fundamental problem*: How does a rock mass relax its state of stress under geostatic conditions? (all-around compression)

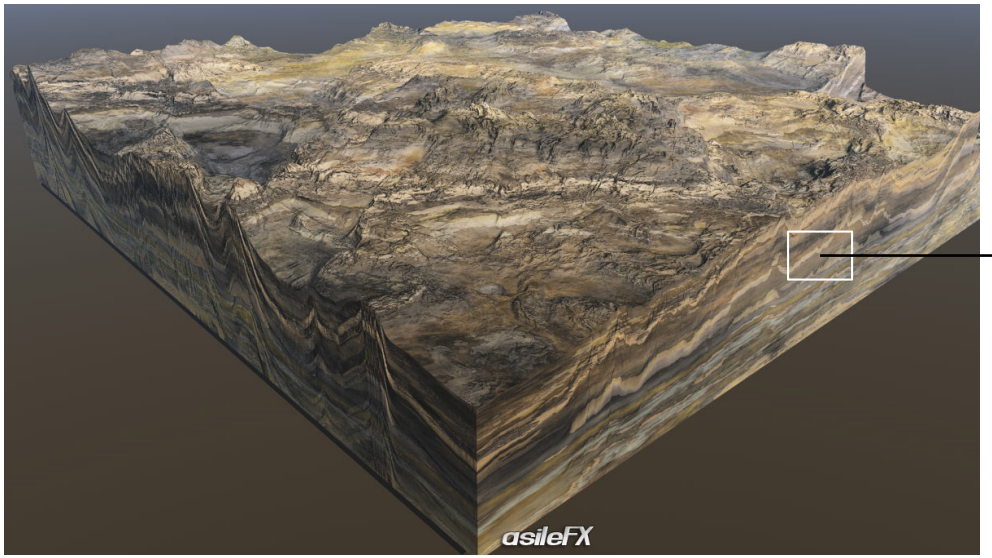

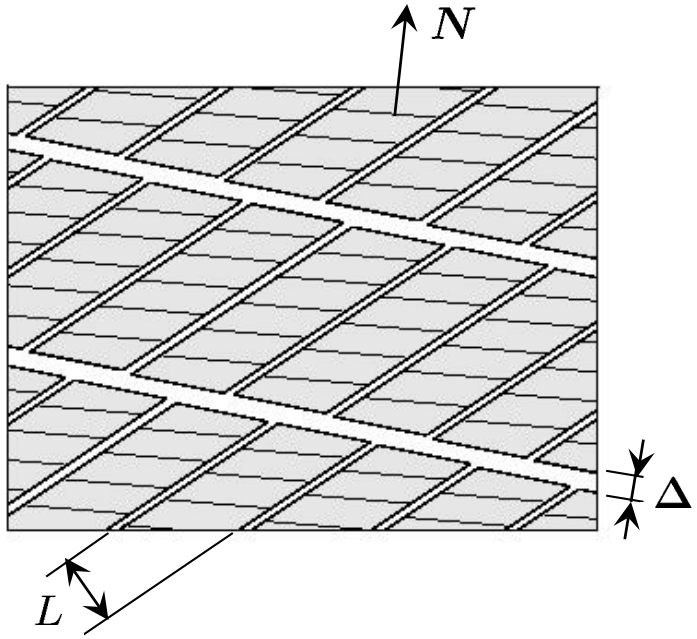

- Mechanisms: i) *Elasticity,* ii) *fracture,* and iii) *friction*
- Optimal fracture pattern: *Nested parallel faults!*

Pandolfi, A., Conti, S. and Ortiz, M., *JMPS,* **54** (2006) 1972-2003.

Recursive (nested) faulting

- Rocks develop *intricate fracture patterns* consisting of almost parallel, almost equidistant, *nested fractures/faults*
- *Recursive (nested) microstructure*, defined by N, Δ and L.

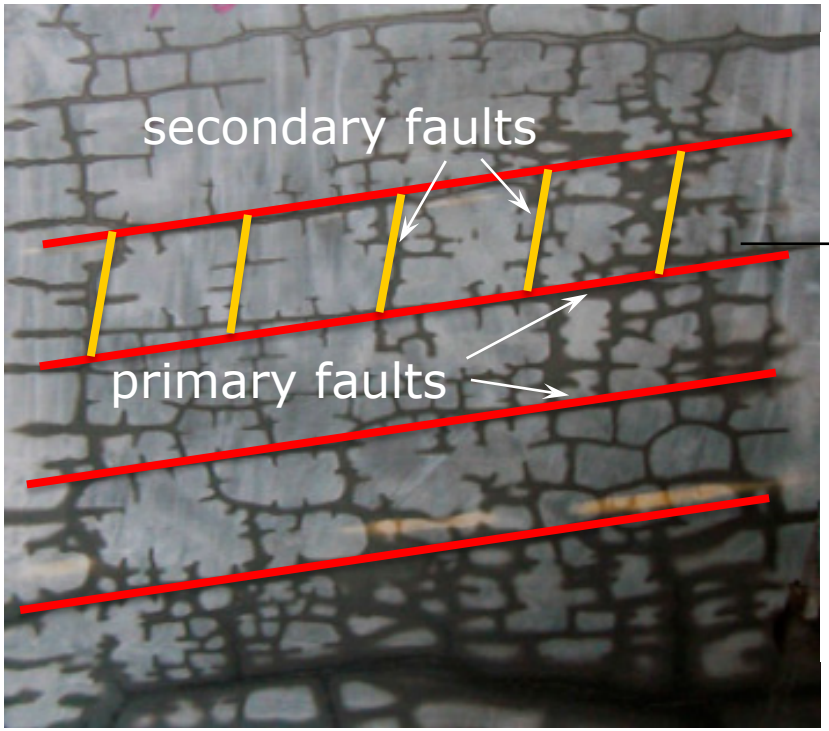

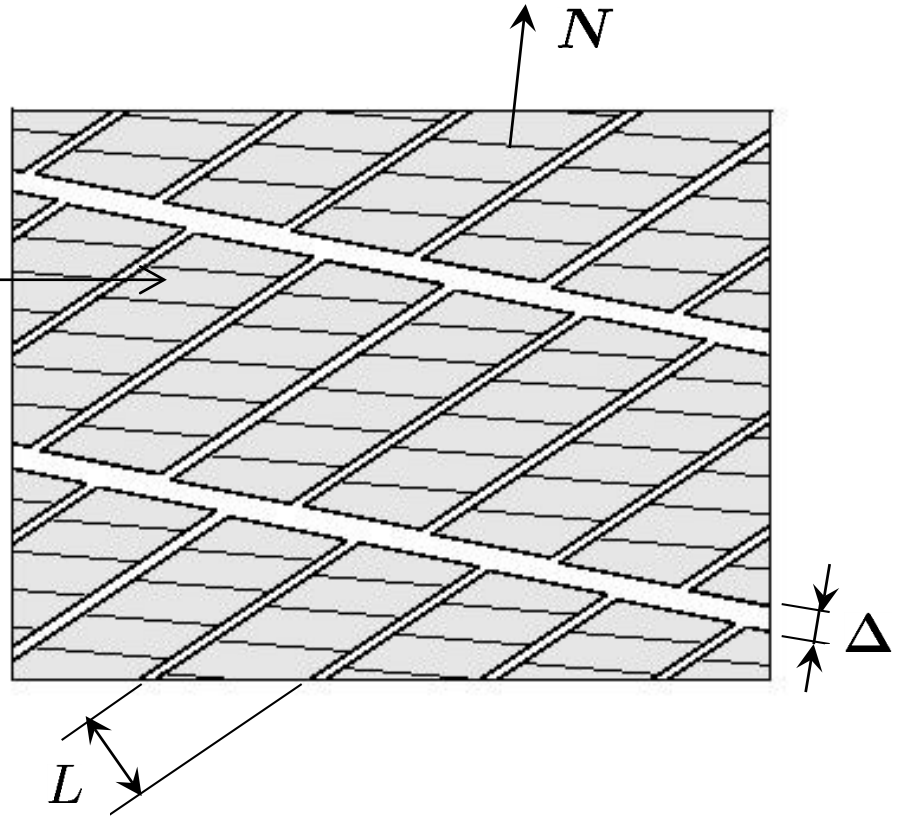

Pandolfi, A., Conti, S. and Ortiz, M., *JMPS,* **54** (2006) 1972-2003.

Mechanics of single family of faults

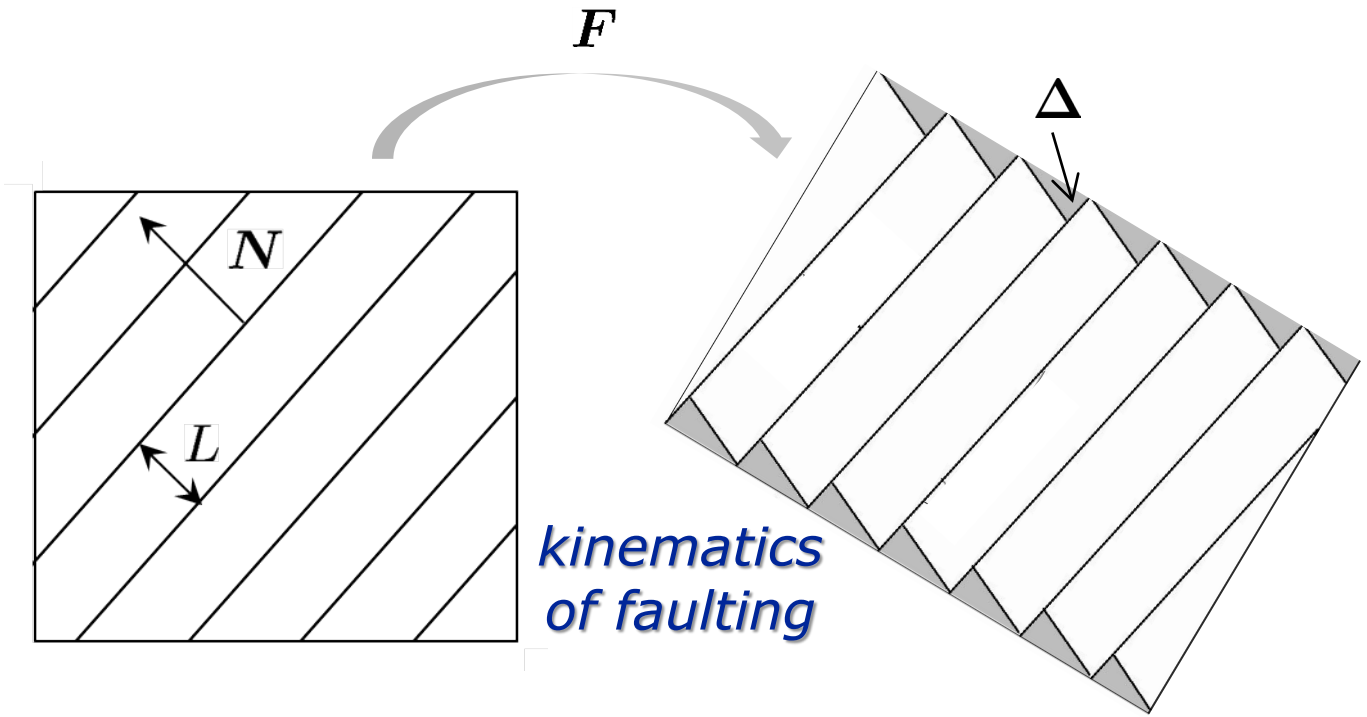

- Incremental minimization of *energy* (finite elasticity) and *dissipation* (cohesive fracture + friction)
- Fault inception: *Maximum tension vs. Mohr-Coulomb*
- Fault spacing, size effect: *Misfit energy* at the boundary

Pandolfi, A., Conti, S. and Ortiz, M., *JMPS,* **54** (2006) 1972-2003.

Recursive faulting construction

- Once the first fault family has developed, the matrix between faults may experience a tensile/shear state resulting in *further faulting* on a sublevel.
- *Nested faulting* of any depth (rank) can be implemented simply by a *recursive call* to the single-family model (supported in C and C++ languages)

$$\mathbf{F} = \mathbf{F}^{(1)}_{\text{mat}}\mathbf{F}^{(1)}_{\text{coh}} \quad \text{Rank-1}$$

$$\mathbf{F}^{(1)}_{\text{mat}} = \mathbf{F}^{(2)}_{\text{mat}}\mathbf{F}^{(2)}_{\text{coh}} \quad \text{Rank-2}$$

$$\mathbf{F}^{(2)}_{\text{mat}} = \mathbf{F}^{(3)}_{\text{mat}}\mathbf{F}^{(3)}_{\text{coh}} \quad \text{Rank-3}$$

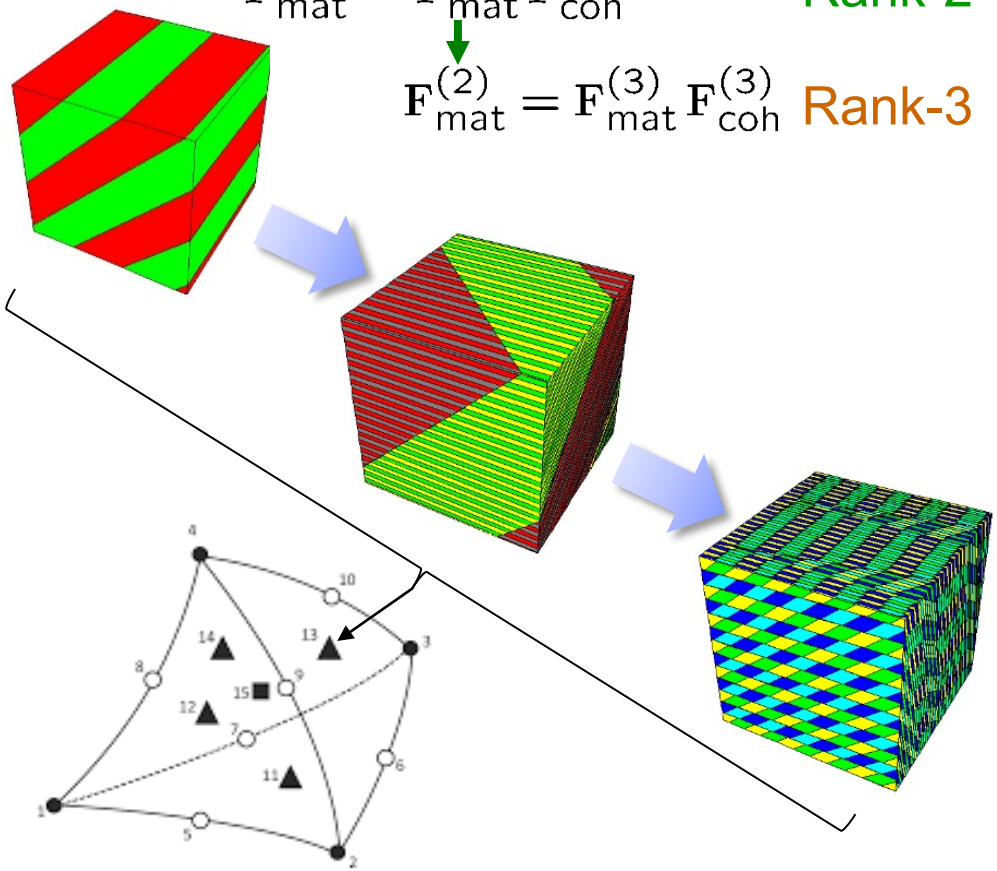

Pandolfi, A., Conti, S. and Ortiz, M., *JMPS,* **54** (2006) 1972-2003.

Localization of damage at macroscale

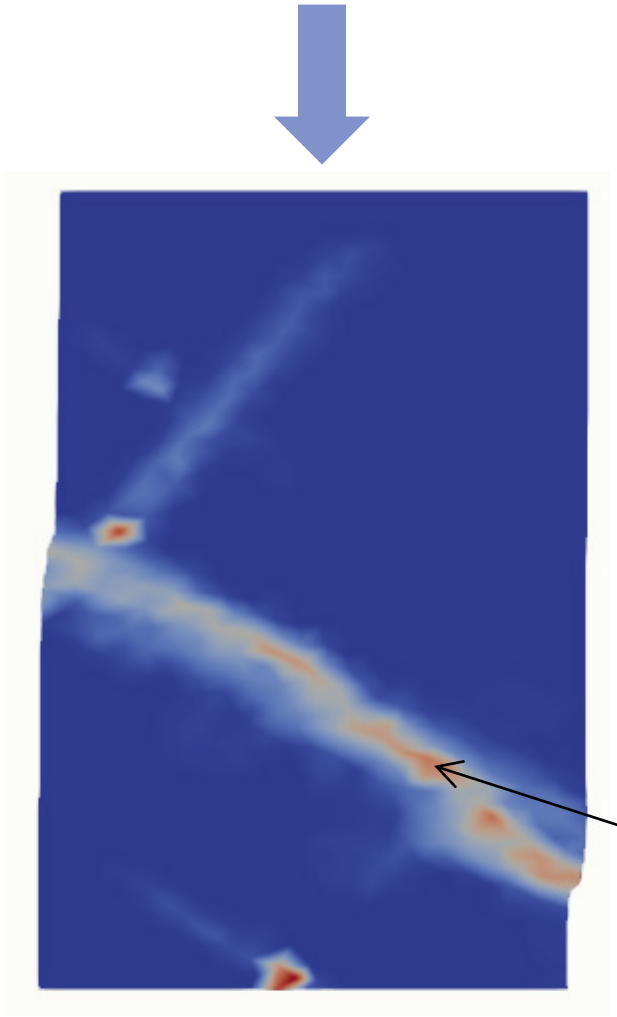

- *Damage can localize* at macroscale (damage bands) as part of *failure mode* of specimen
- Orientation of *micro-fractures* differs from that of macroscopic damage bands
- Orientation of both macroscopic damage bands and distribution of micro-fractures are independent outcomes of the analysis

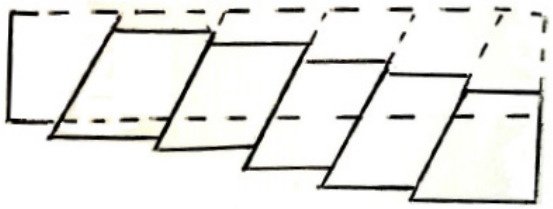

Micro-fracture pattern in damage band

Plane strain biaxial compression test

Damage-enhanced permeability

- *Recursive-faulting* construction characterizes both *average macroscopic behavior* and *fine structure* at the microscale
- Can use computed microscopic fracture geometry/deformation to predict *permeability*

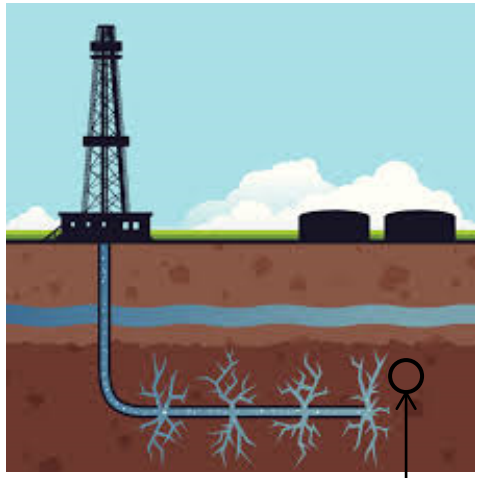

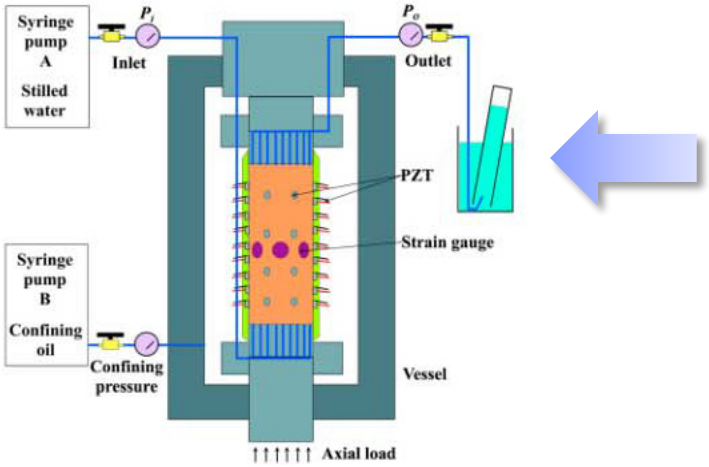

Lei et al., *Geophys. Res. Let.*, **38**, L24310, 2011

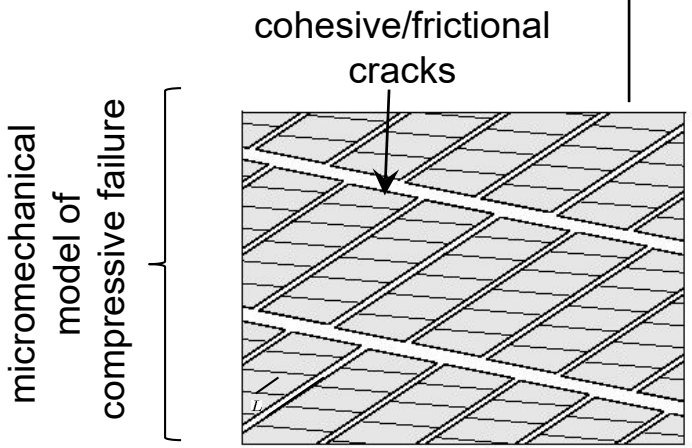

Pandolfi, A., Conti, S. and Ortiz, M., *J. Mech. Phys. Solids,* **54**: 1972-2003, 2006

Damage-enhanced permeability

- *Fluid-to-solid*: *Terzaghi*'s effective stress principle
- *Solid-to-fluid*: Permeability due to fracture (*Couette flow*):

$$\kappa^{\mathrm{f}} = \sum_{k=1}^{Q} \frac{\Delta_N^k}{L^k + \Delta_N^k} \frac{{\Delta_N^k}^2}{12} \left(\boldsymbol{I} - \boldsymbol{N}^k \otimes \boldsymbol{N}^k \right)$$

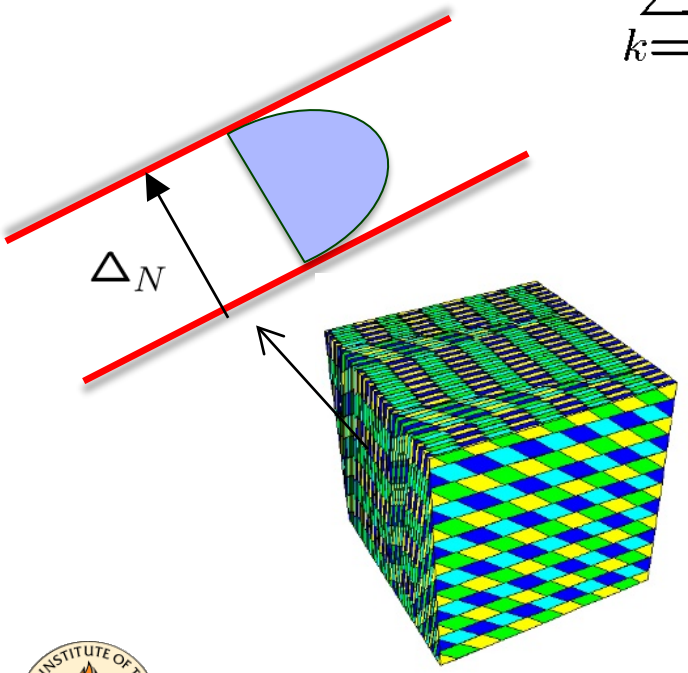

fault-orientation dependence
(anisotropic permeability…)

fault-opening dependence
(effect of stress, pressure, friction…)

fault-density dependence
(specific fracture energy, size effect…)

M.L. De Bellis, G. Della Vecchia, M. Ortiz, A. Pandolfi,
Engineering Geology, **215** (2016) 10-24

Experimental validation – Impact

- Kolsky-bar dynamic impact experiments on *AlN cylindrical specimens* with shrink-fit *steel sleeve confinement*[1]
- *Confinement increases the ductility* of the specimen, both in static and in dynamic case.

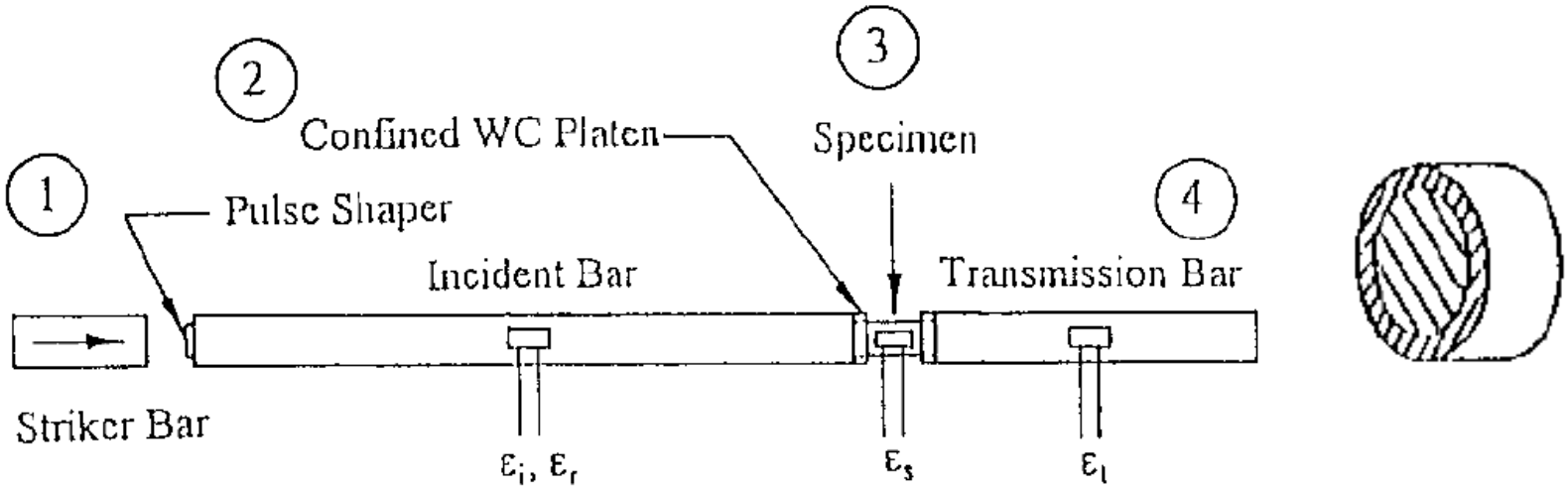

[1]W. Chen and G. Ravichandran, *JACS*, **79**(3) (1996) 579-584

Experimental validation – Impact

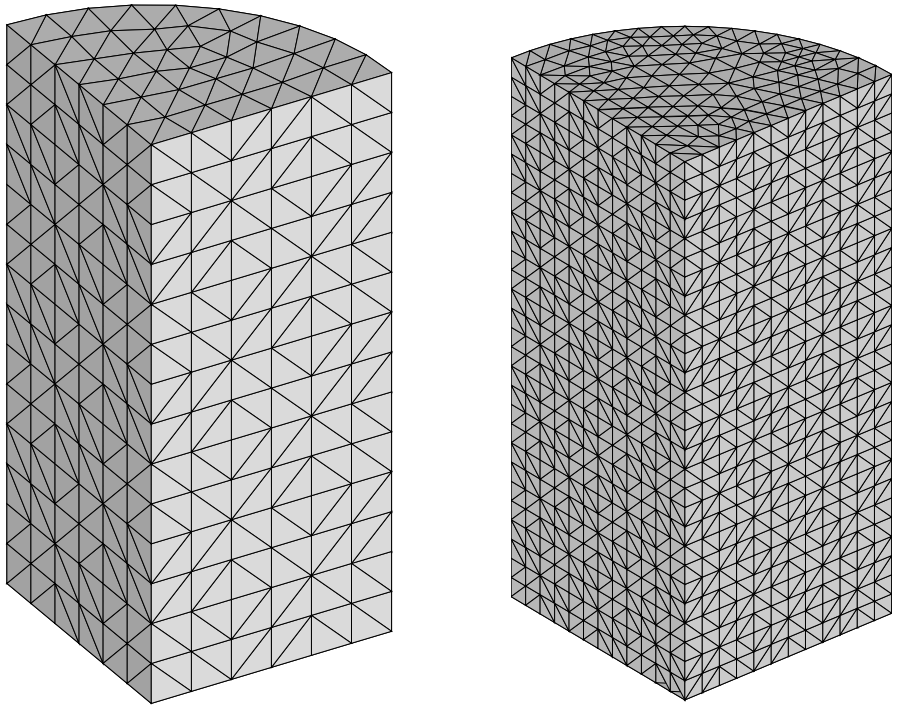

$E =$ 310 GPa

$\nu =$ 0.237

$T_c =$ 180 MPa

$G_c =$ 162 N/m

$\beta^2 =$ 12

$L_0 / L_c =$ 100

$\rho =$ 3200 kg/m^3

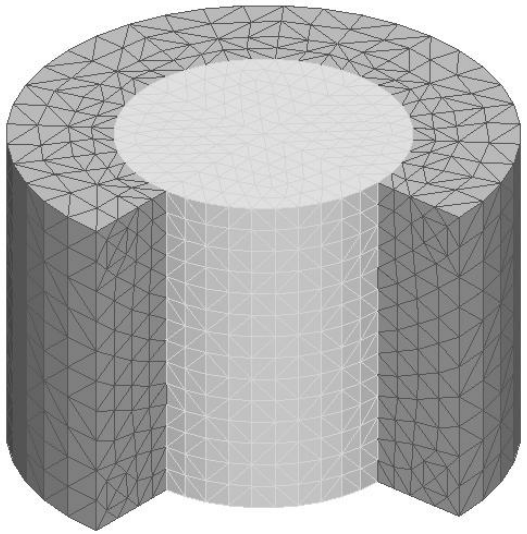

- *Tetrahedral FE meshes* of AlN specimen and steel sleeve
- *Two mesh sizes* to verify mesh-size insensitivity of calculations

Pandolfi, A., Conti, S. and Ortiz, M., *JMPS,* **54** (2006) 1972-2003.

Experimental validation – Impact

Experiments (Chen and Ravichandran '96)

Top view

Cross Section

Bottom view

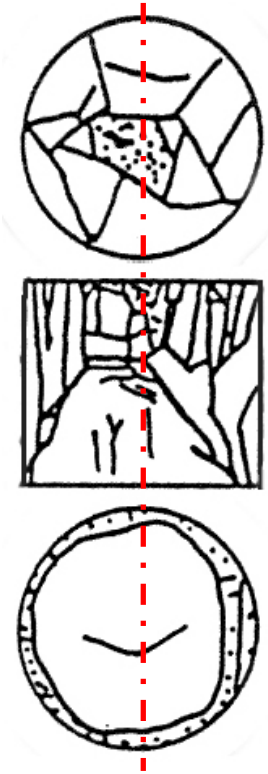

Damage contour levels Cross section

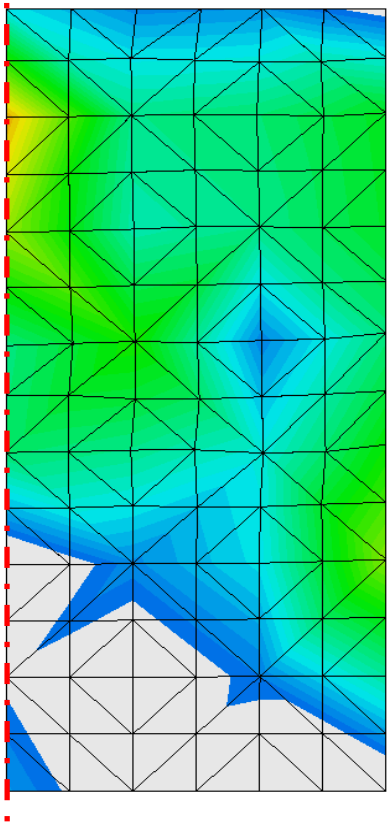

Planes of fracture (black) and opening (red) Cross section

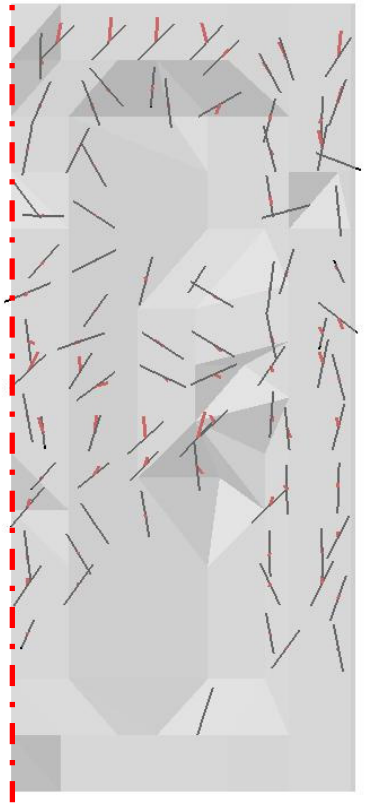

Top view

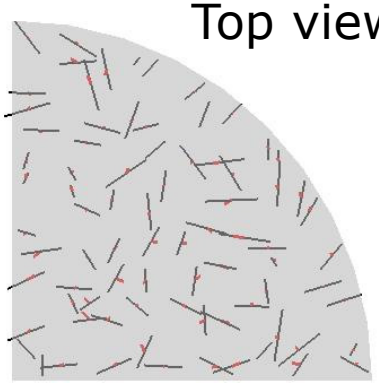

Bottom view

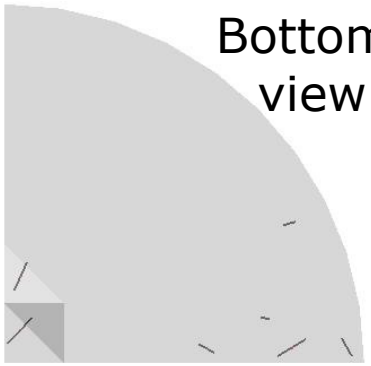

Pandolfi, A., Conti, S. and Ortiz, M., *JMPS,* **54** (2006) 1972-2003.

Experimental validation – Impact

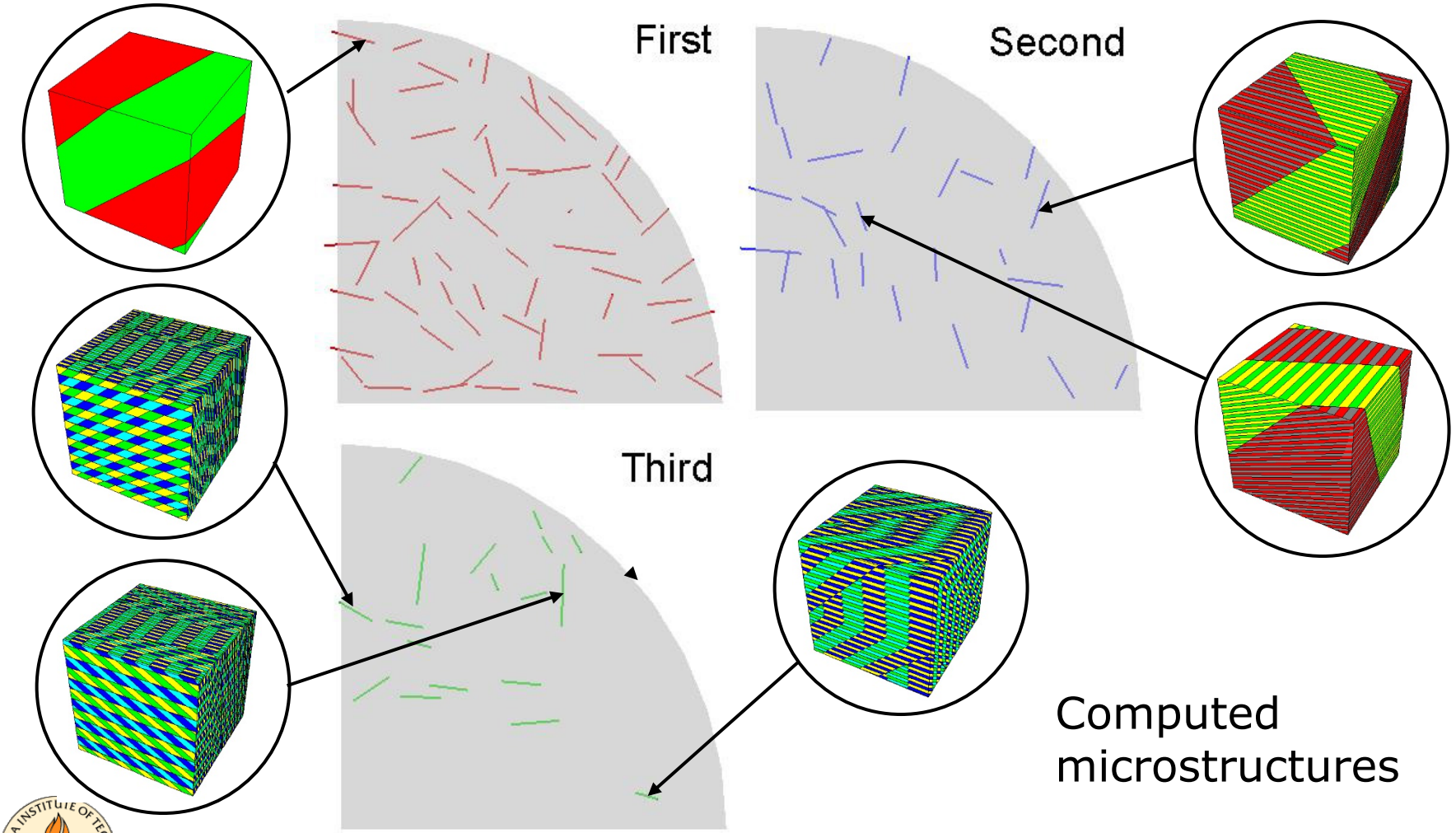

Pandolfi, A., Conti, S. and Ortiz, M., *JMPS,* **54** (2006) 1972-2003.

Experimental validation – Impact

Comparison with experiments[1]

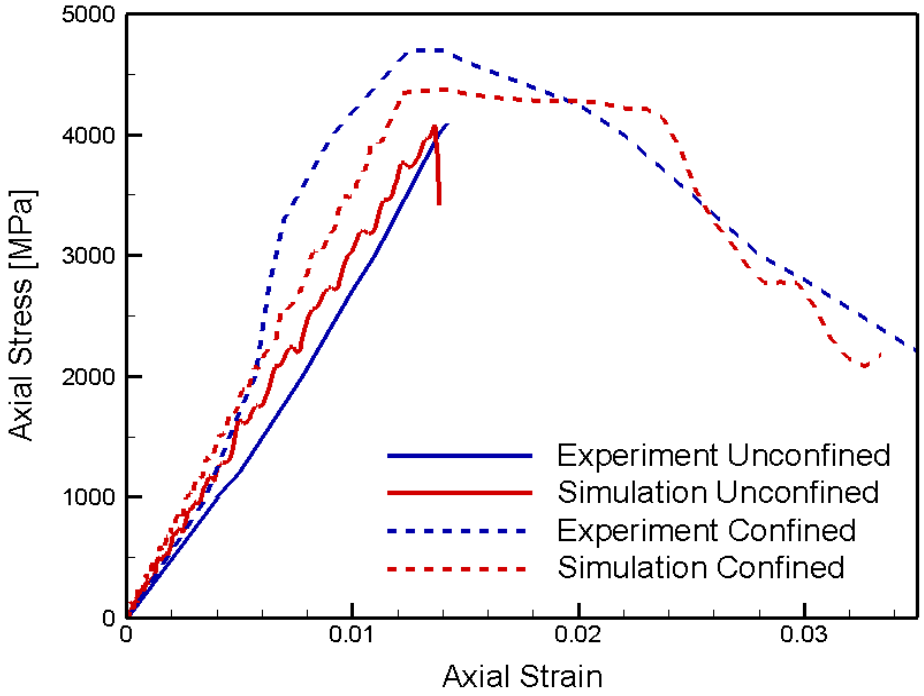

Mesh size analysis

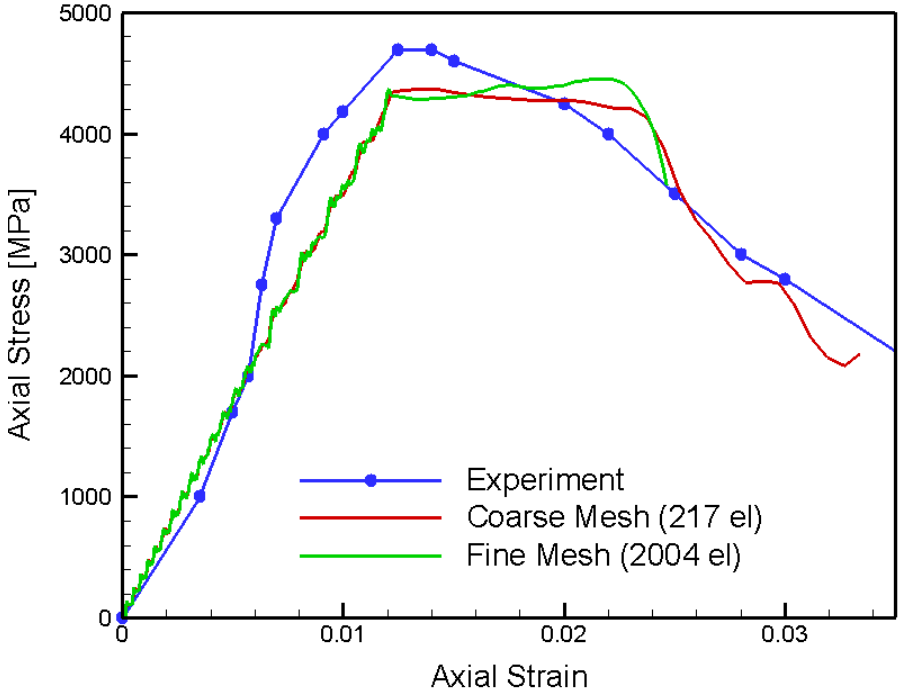

- Model captures *brittle-to-ductile transition*
- Model results are *mesh-size insensitive*

[1]W. Chen and G. Ravichandran, *JACS*, **79**(3) (1996) 579-584.
Pandolfi, A., Conti, S. and Ortiz, M., *JMPS*, **54** (2006) 1972-2003.

Experimental validation – Triaxial test

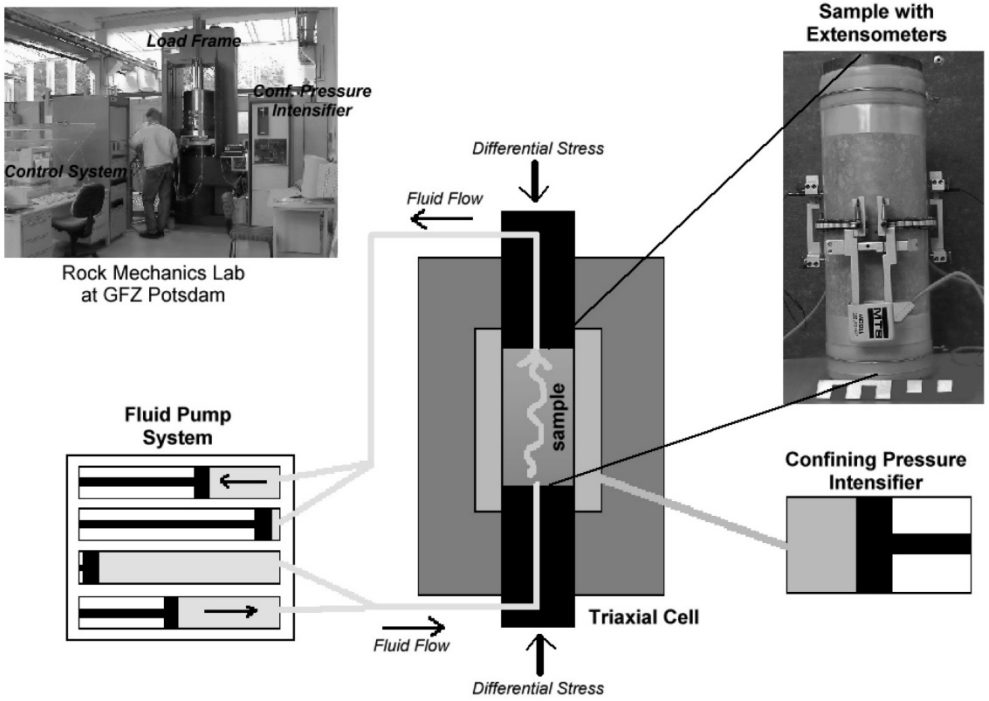

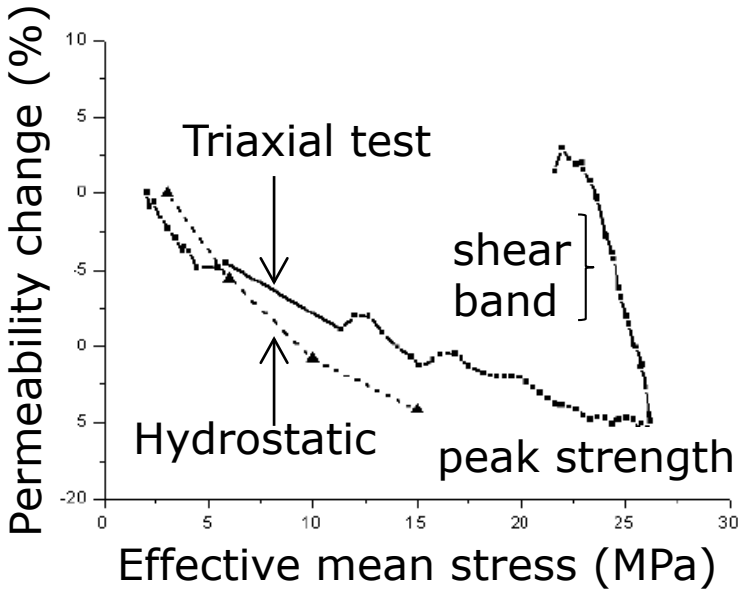

J. Heiland, *Hydrogeology Journal*, **11**:122-141, 2003.

Experimental validation – Triaxial test

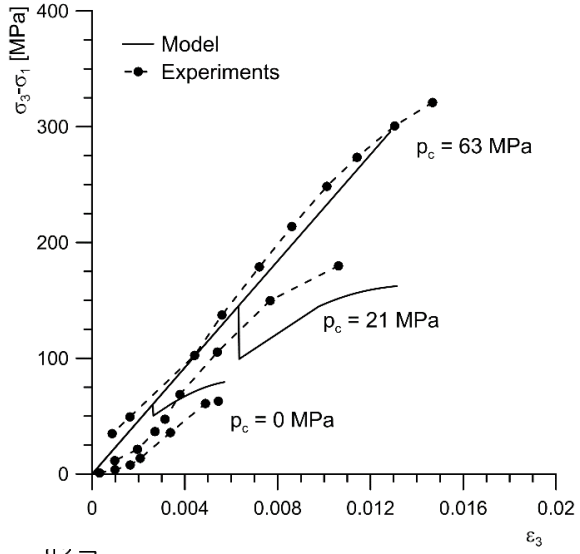

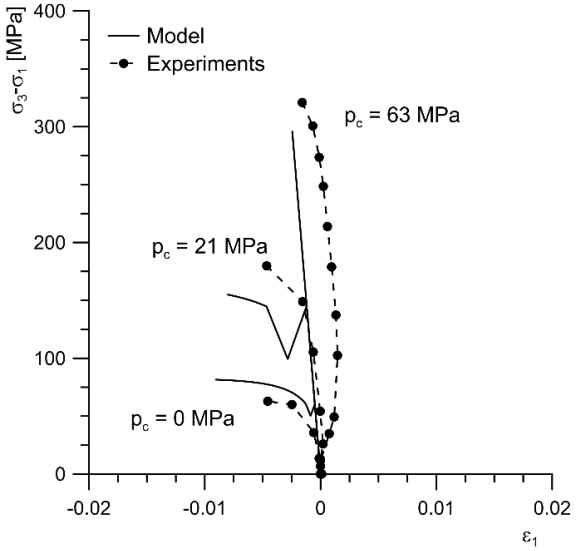

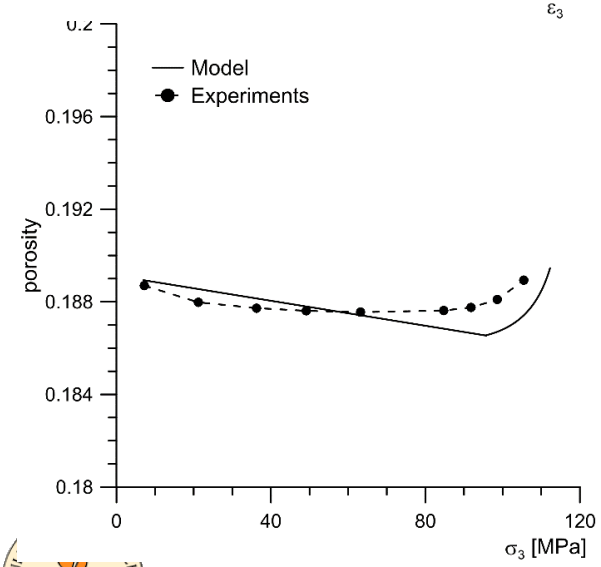

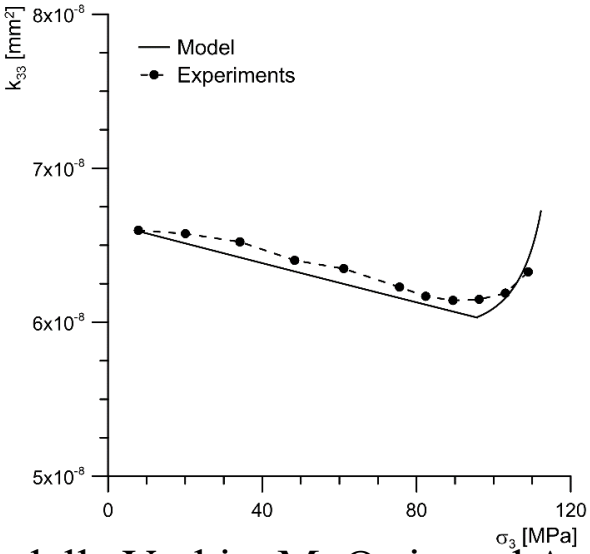

- Experiments on berea sandstone [Morita *et al*., 1992]
- Axial and radial stress-strain curves
- Microstructures:

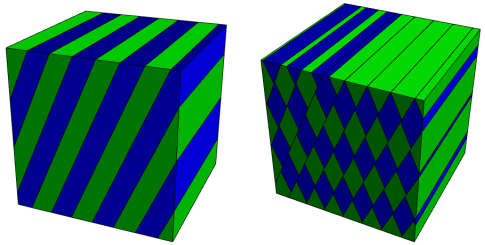

- Curves of porosity and permeability in axial direction

M.L. de Bellis, G. della Vechia, M. Ortiz and A. Pandolfi, *JMPS*, **104** (2017) 12-31.

Experimental validation – Triaxial test

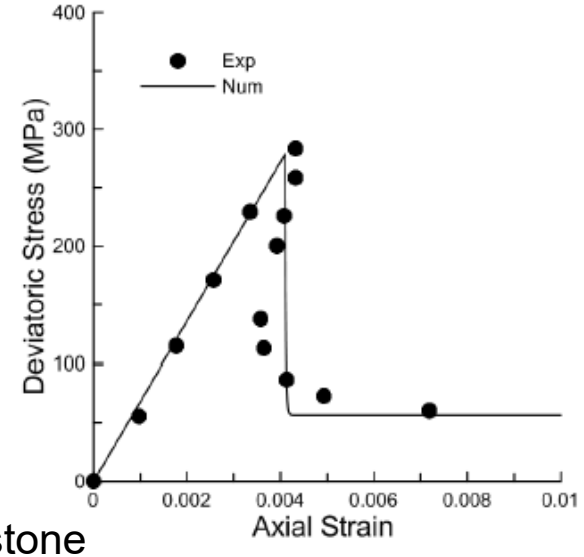

Inada sandstone
(Kiyama et al, 1996)

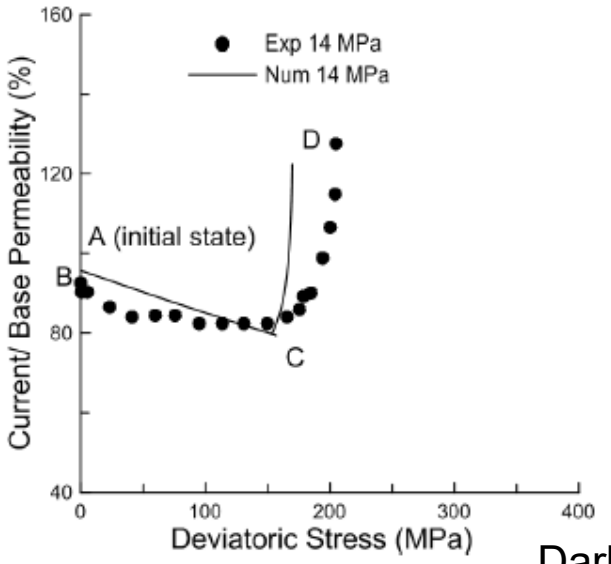

Darley dale sandstone
(Mordecay, 1970)

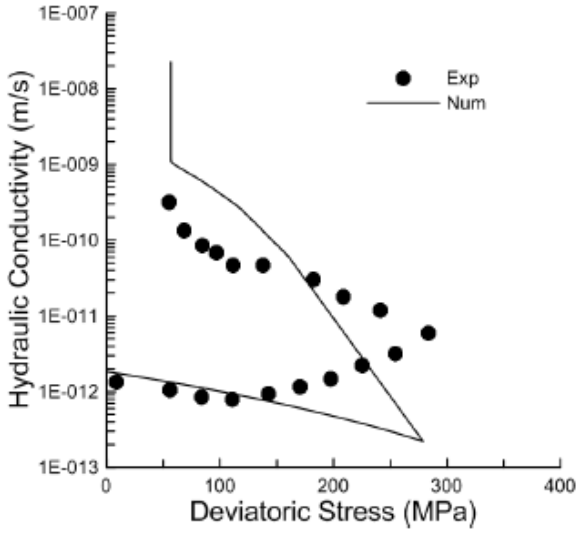

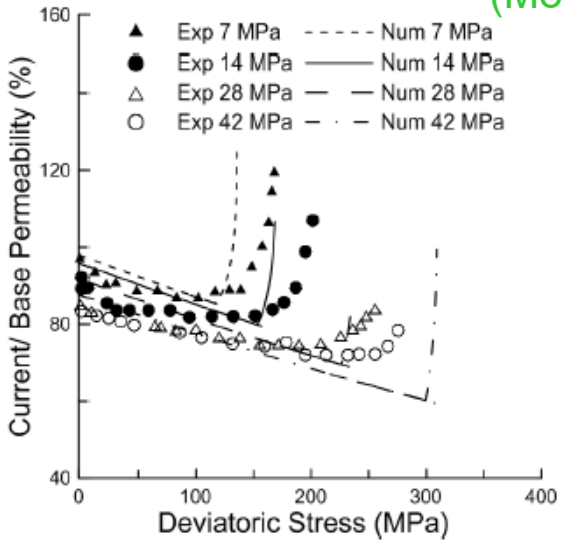

Experimental validation – Triaxial test

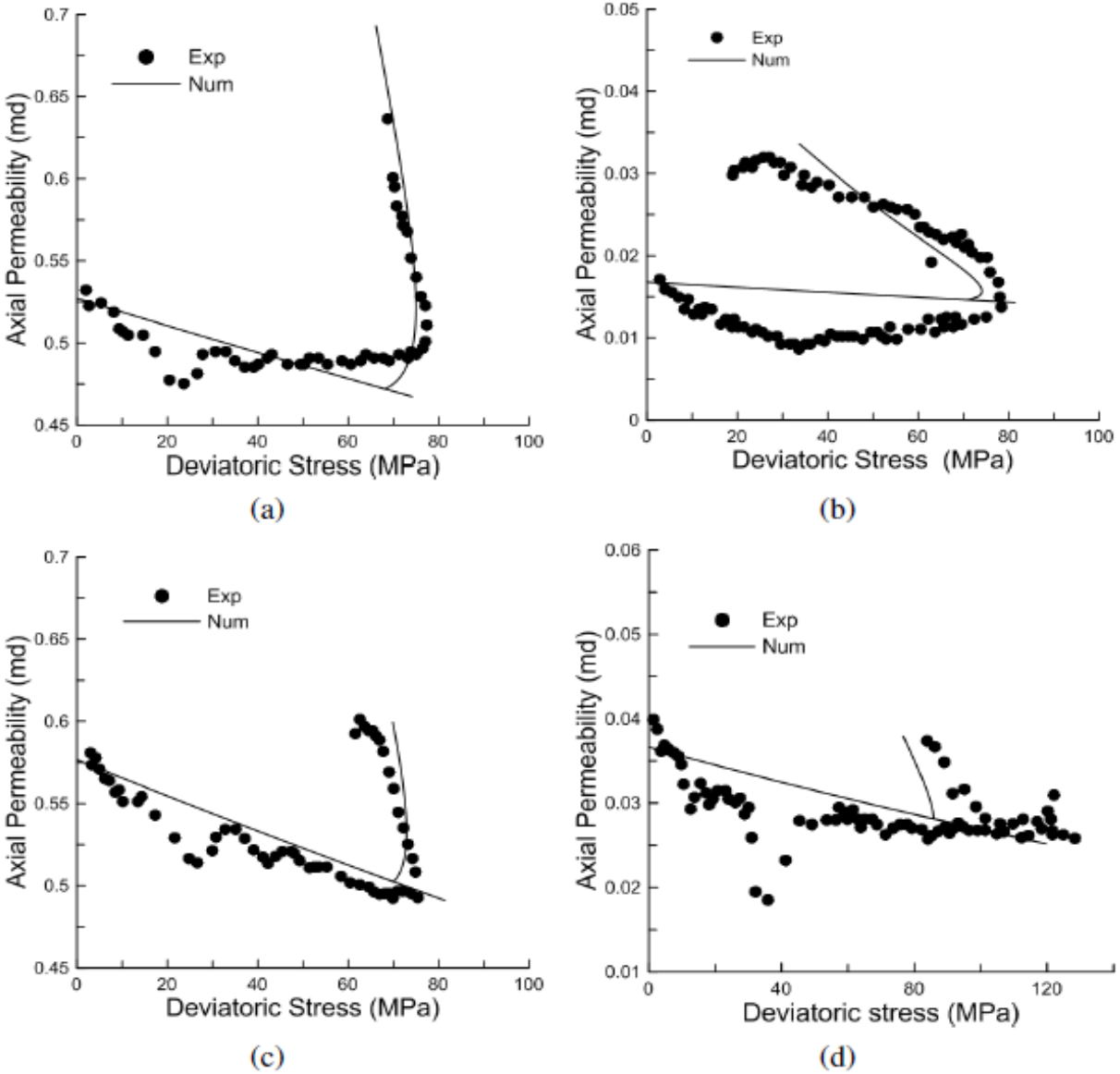

Experiments on Flechinger sandstone, with increasing confinement [Heiland, 2003]

Experimental validation – Triaxial test

Westerly granite

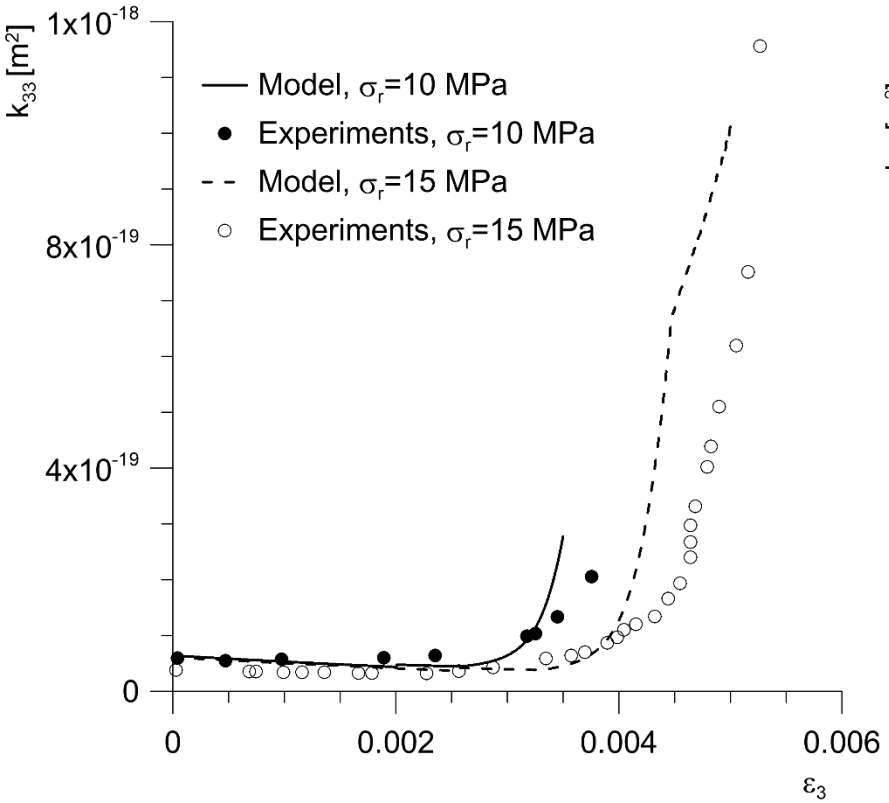

Cerro Cristales granodiorite

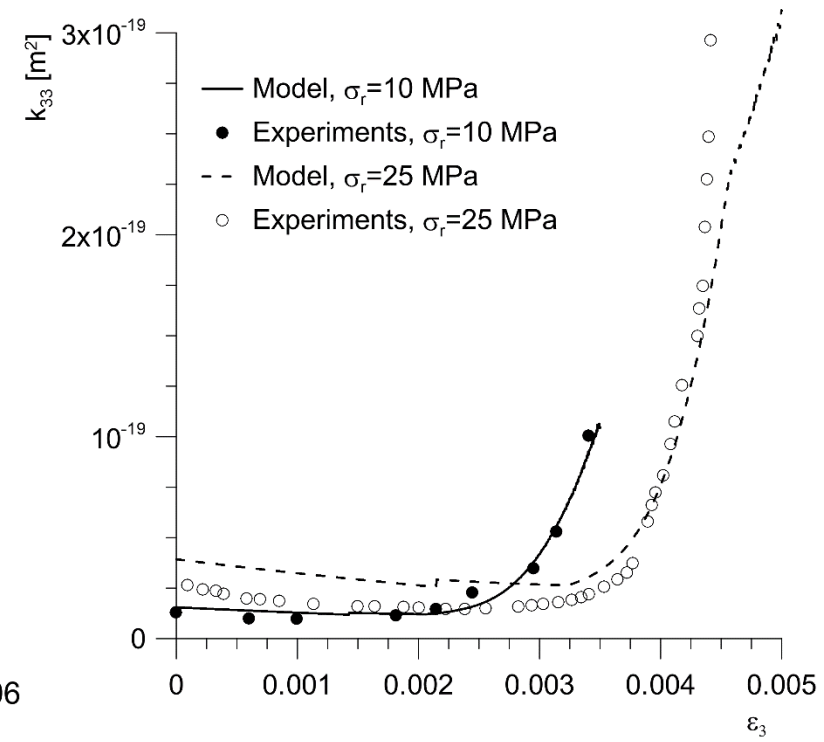

- Experiments on low porosity rocks [Mitchell and Faulkner, 2008]

M.L. de Bellis, G. della Vechia, M. Ortiz and A. Pandolfi, *JMPS*, **104** (2017) 12-31.

Validation: Cement block, triaxial loading

- Compressed cement block
- Pressurized fluid in small cylindrical cavity at center of specimen
- Fluid-flow control
  [Athavale & Miskimins, 2008]
  σ_z = 24.2 MPa
  σ_x = 17.3 MPa
  σ_y = 10.4 MPa

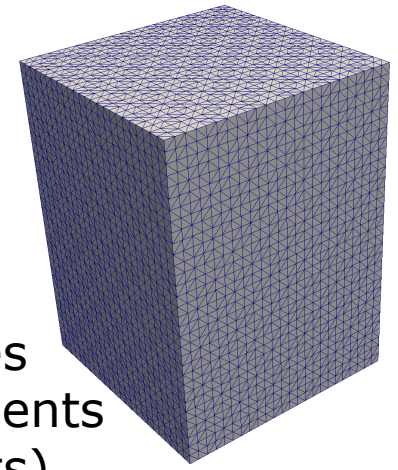

38,000 nodes
28,000 elements
(10-node tets)

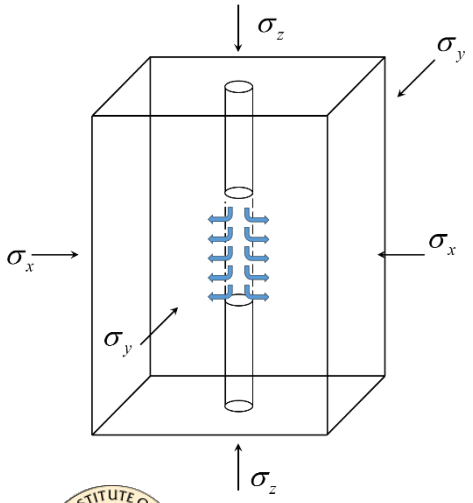

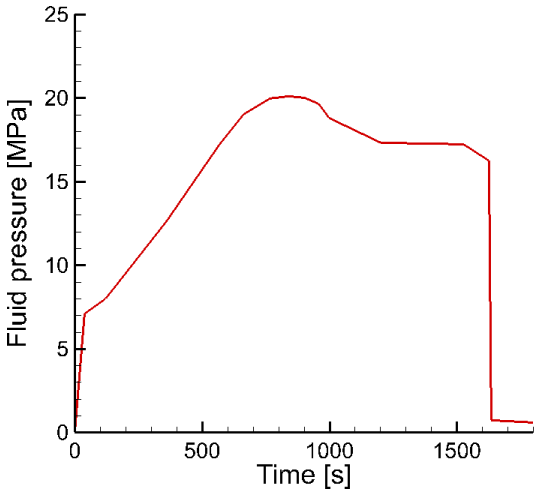

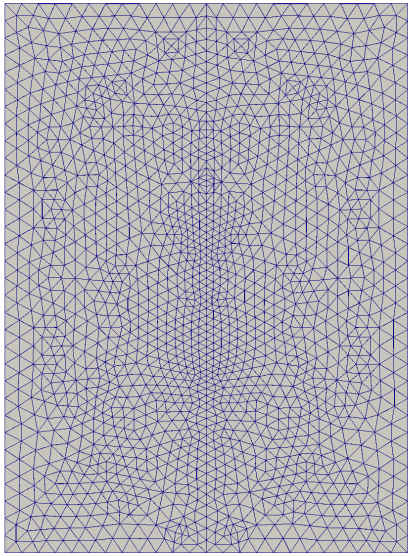

M.L. de Bellis, G. della Vechia, M. Ortiz and A. Pandolfi, *JMPS*, **104** (2017) 12-31.

Validation: Cement block, triaxial loading

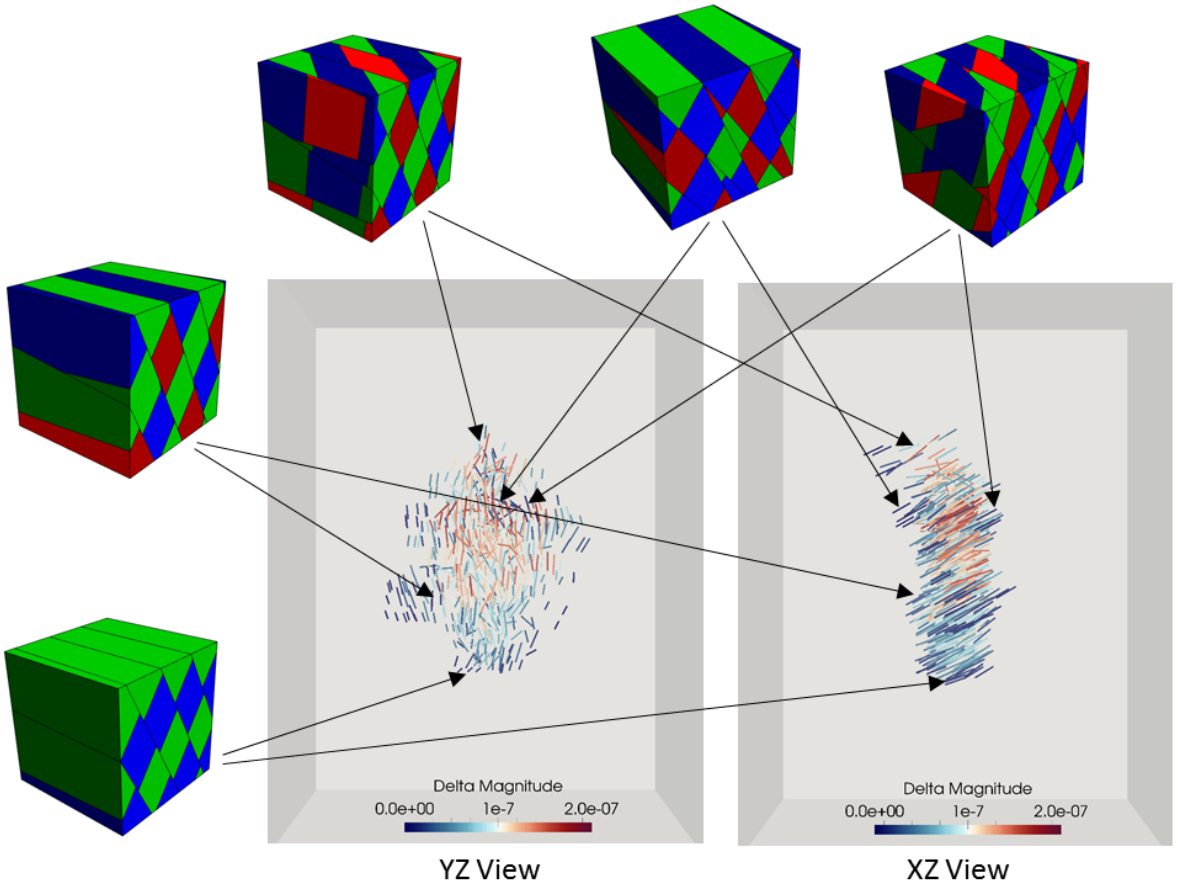

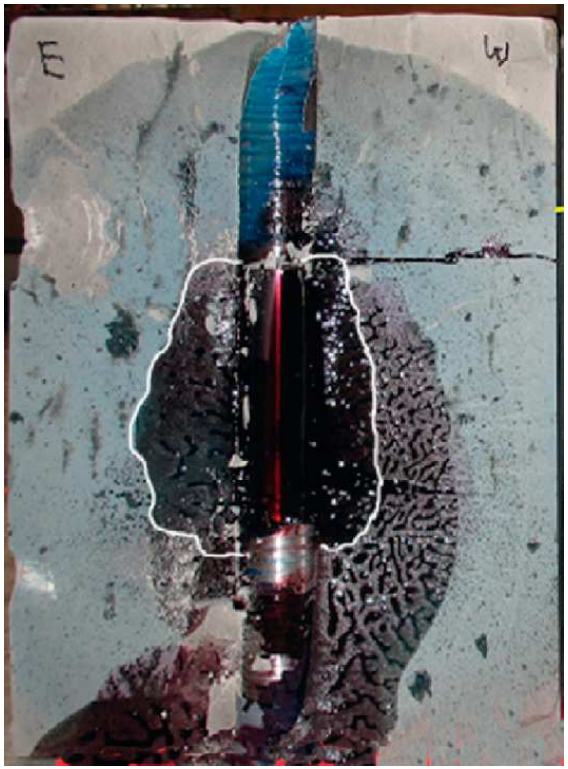

- Colored lines: Fault normal, sliding displacement
- Representative rank-2 and rank-3 microstructures
- Faults form according to *Mohr–Coulomb criterion*

Validation: Cement block, triaxial loading

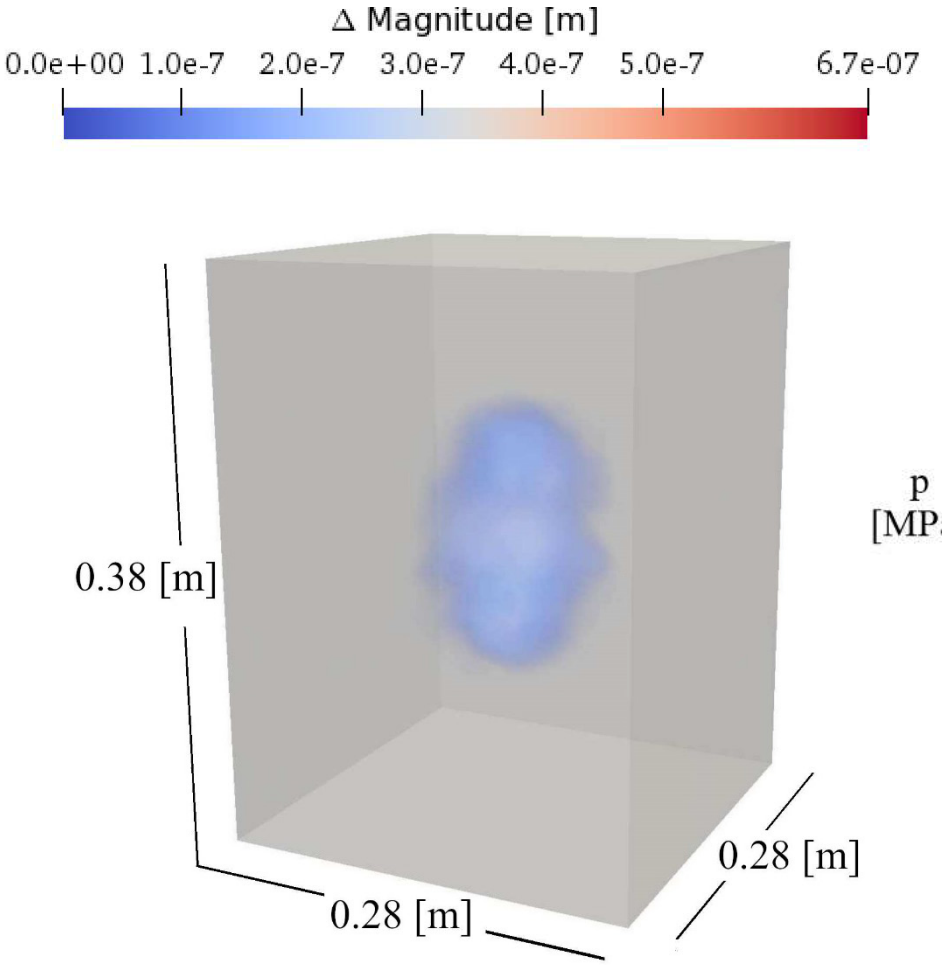

Fault sliding displacement

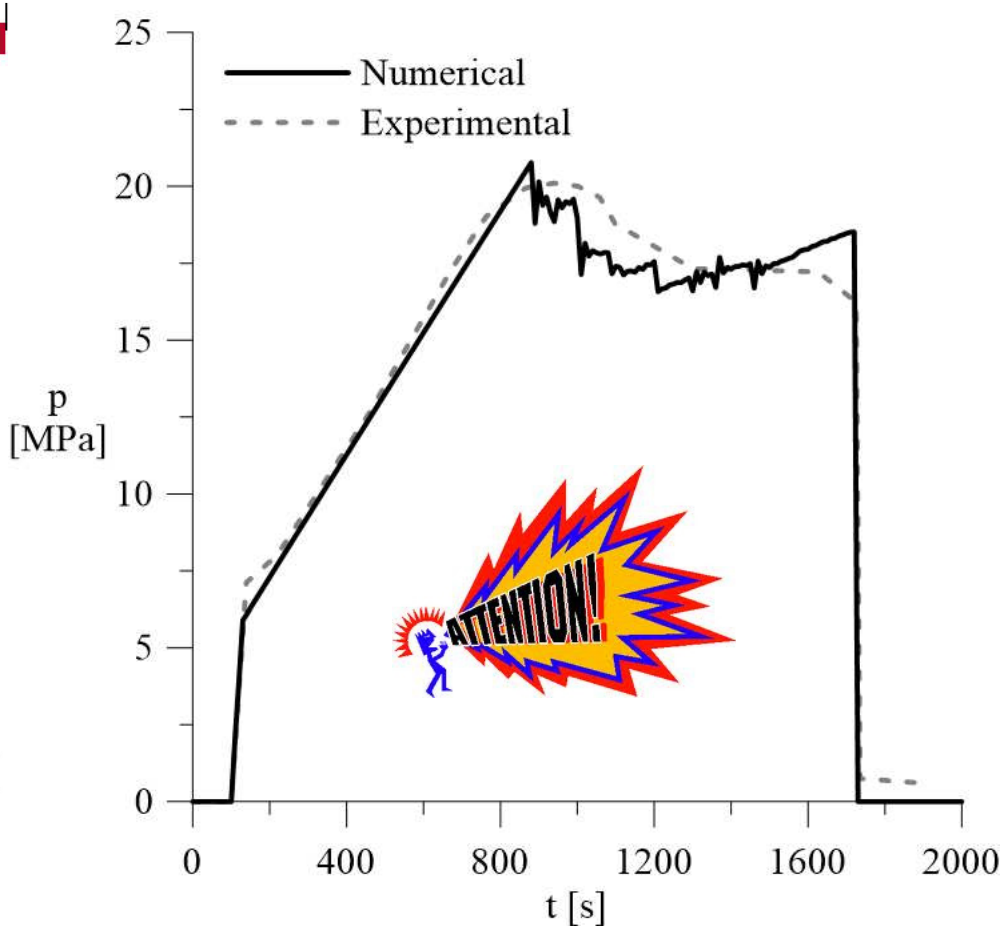

Pressure history

Application: Borehole excavation (dry)

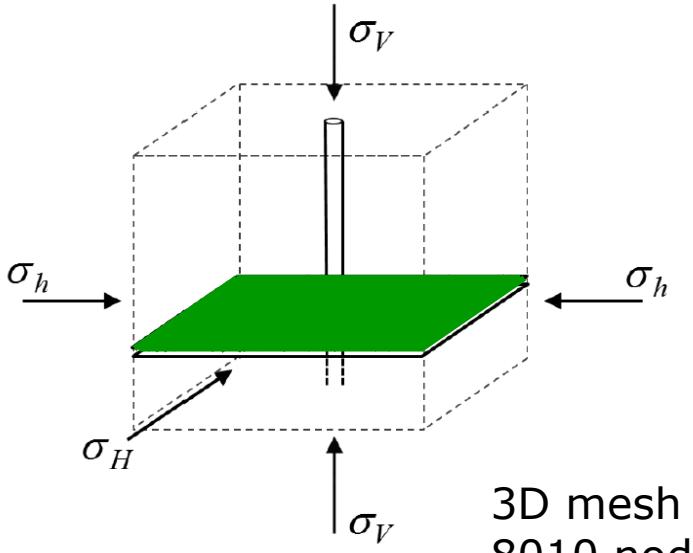

- 2 m diameter *vertical borehole* excavation in *dry rock*
- 10 x 10 m field, at a depth of 10 m [Lisjack et al, JRMMS 2014]

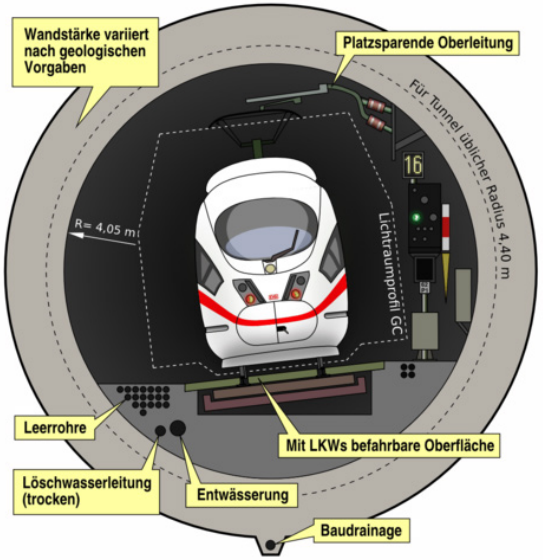

Verringerter Tunnelquerschnitt mit Radius 4,05 m

3D mesh
8010 nodes
36086 elements

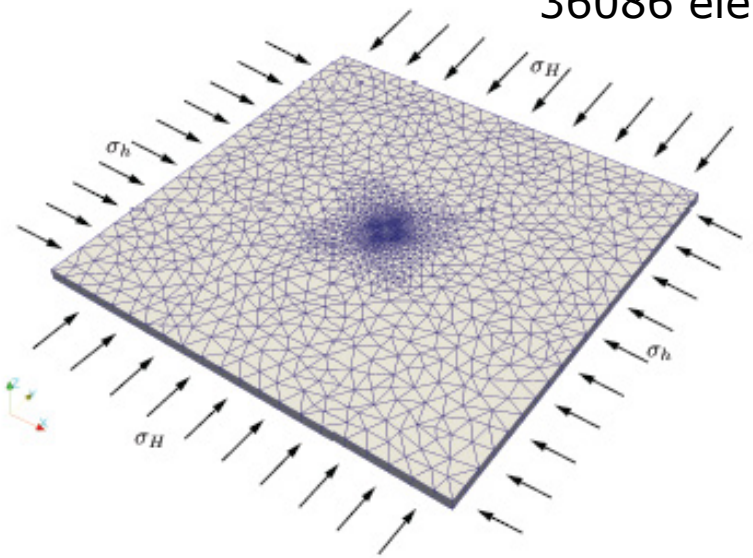

- *Stuttgart 21*, special cross-section in the lower part of the *Filder Tunnel*.

Michael Ortiz
IWS 12/08/20

Application: Borehole excavation (dry)

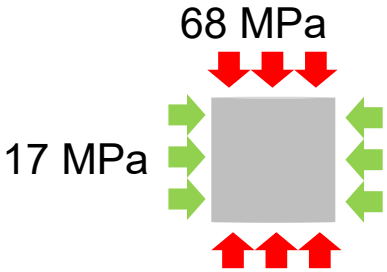

Larger anisotropic stress in the horizontal plane for the intact mass ($K_0 = 4$)

Max stress distribution at the first step of excavation

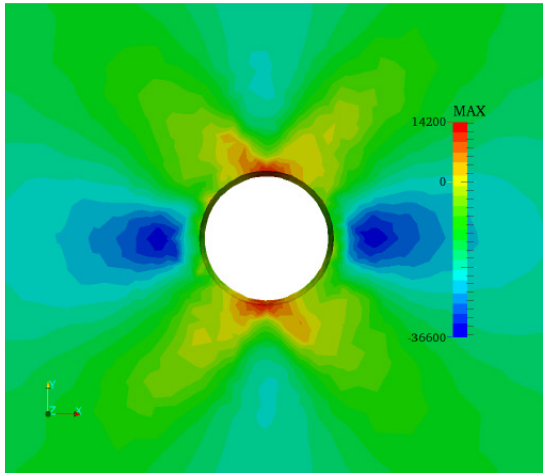

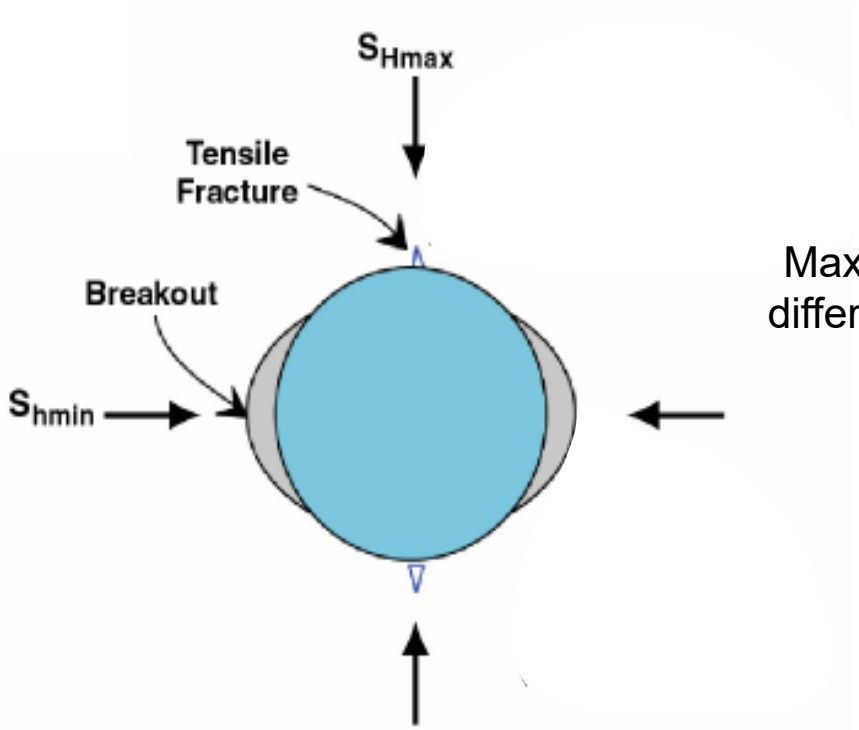

Max-min stress difference at the first step of excavation

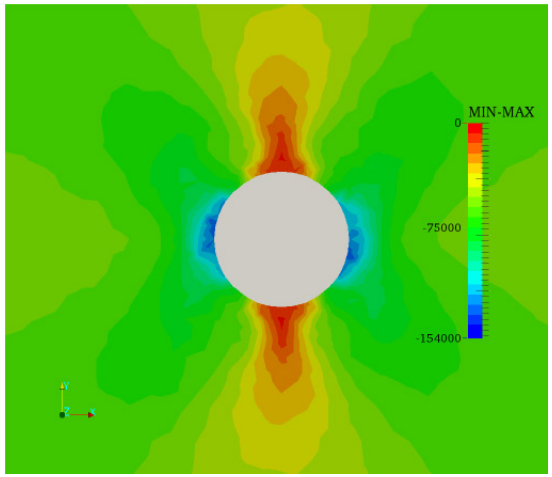

Michael Ortiz
IWS 12/08/20

Application: Borehole excavation (dry)

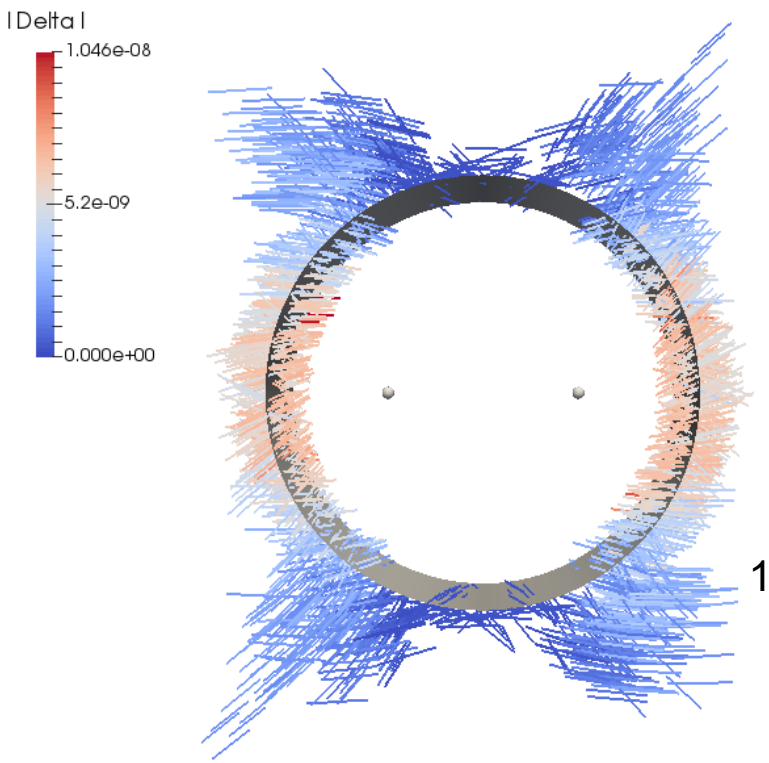

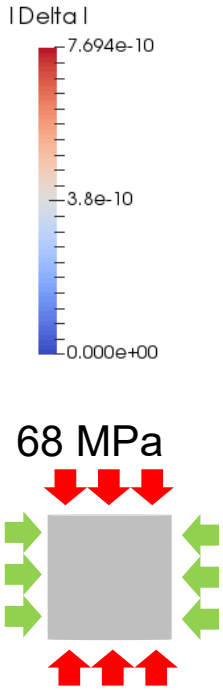

- Arrows oriented as N and colored as Δ

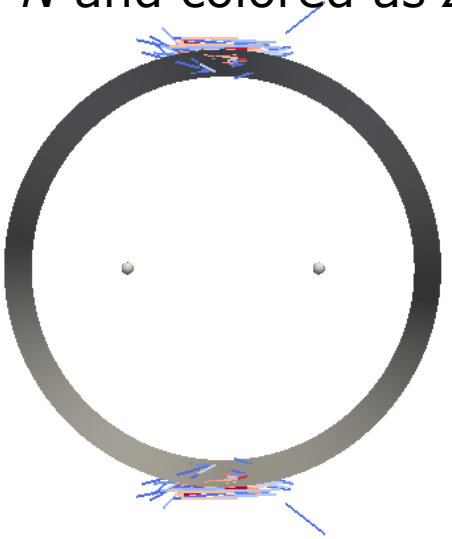

Shear cracks

Tensile cracks

- Computed shear and tensile fracture patterns
- *Diffuse yielding* (sliding cracks) at 45 degrees
- *Splitting* normal to maximum deviatoric tension

Application: Fracking simulation

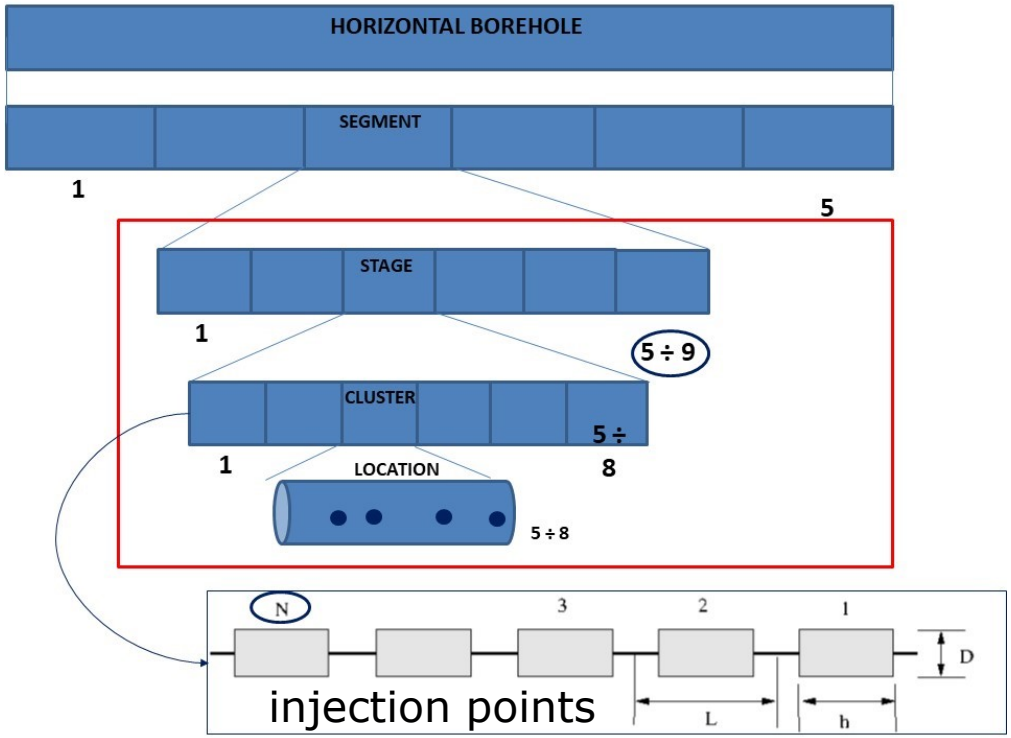

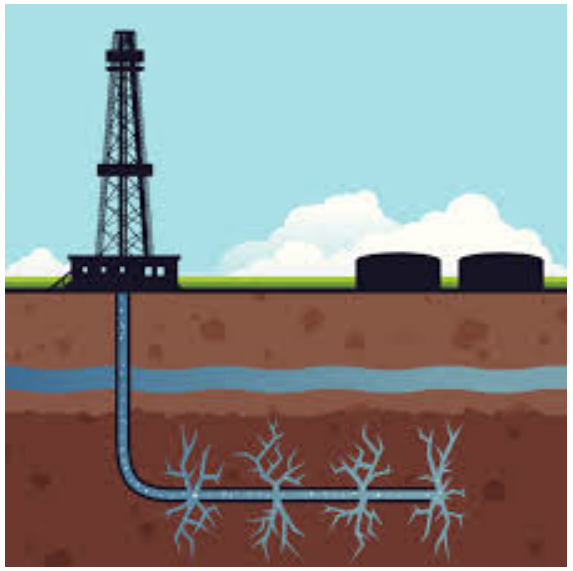

Horizontal borehole

- Each *horizontal borehole* is 1–1.5 miles long and comprises 40–75 *stages* (individual pump treatment).
- A stage comprises 4, 8 or 12 shorter perforated *clusters* which span 250 ft.

Michael Ortiz
IWS 12/08/20

Example: 1 borehole, 8 injections

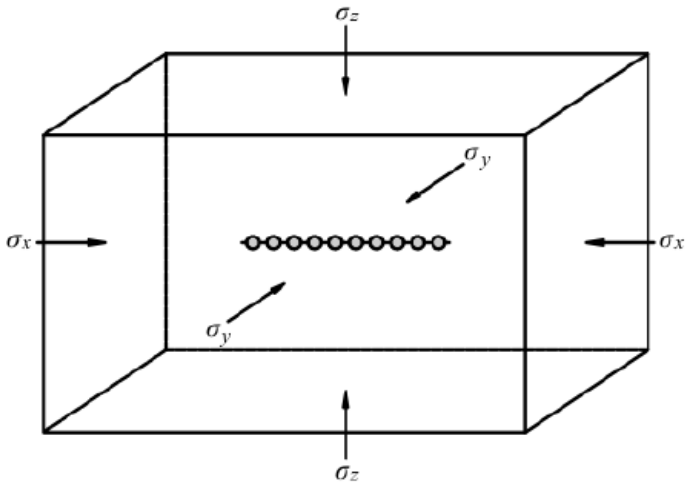

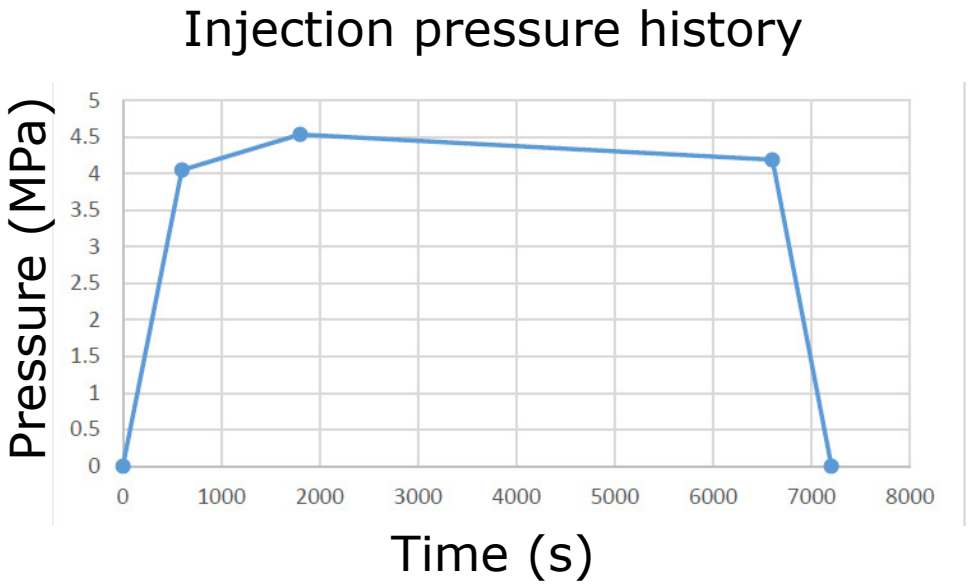

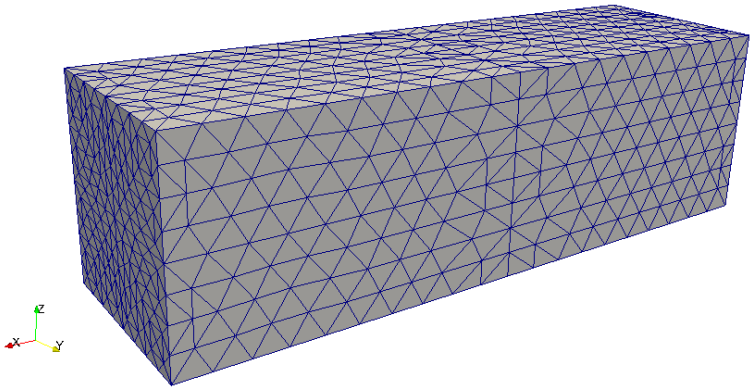

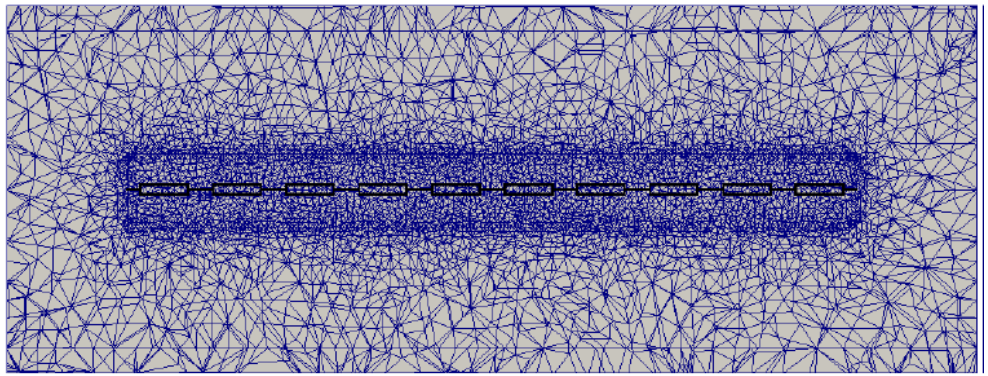

Michael Ortiz
IWS 12/08/20

Example: 1 borehole, 8 injections

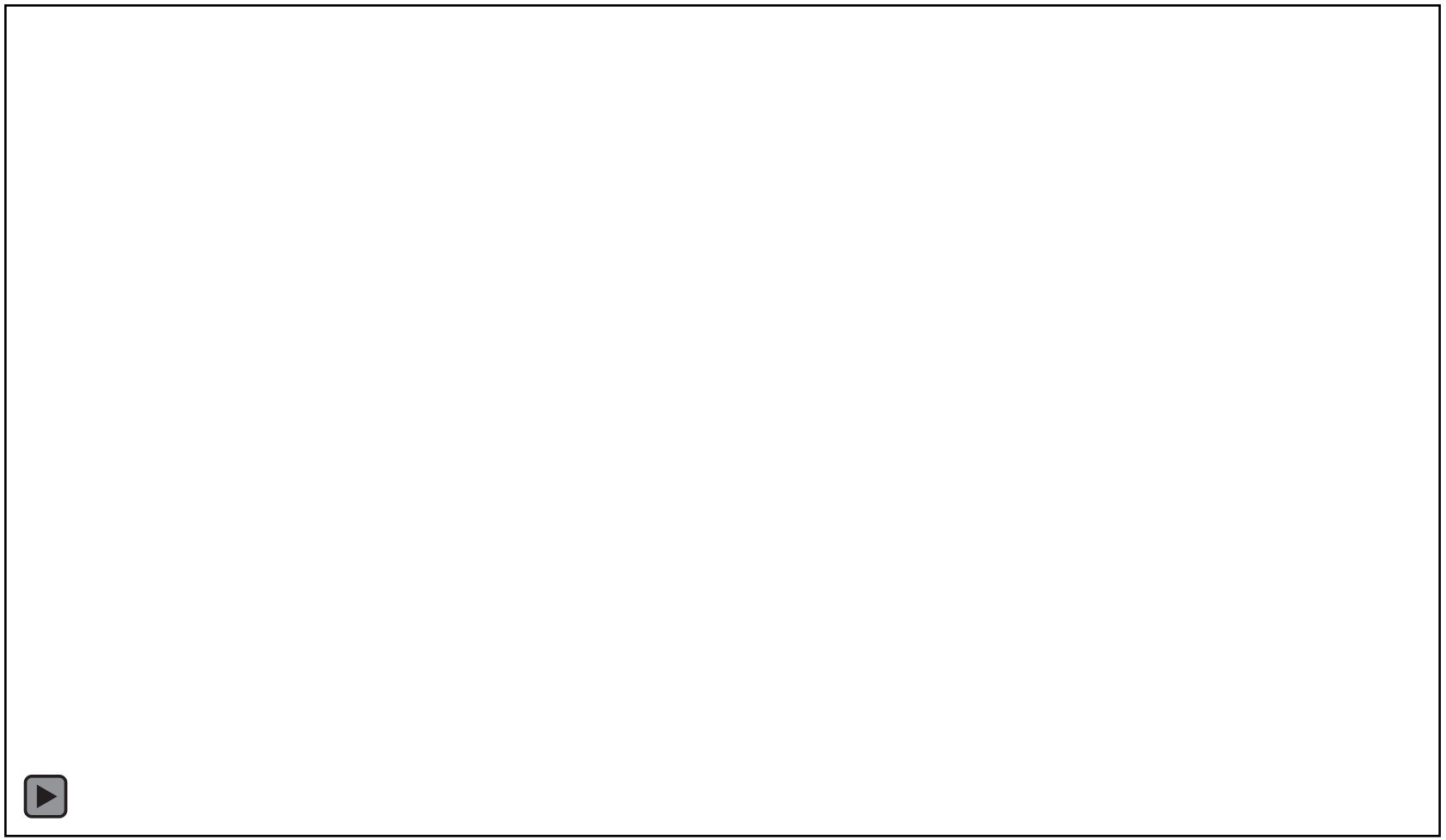

Stress history

Example: 1 borehole, 8 injections

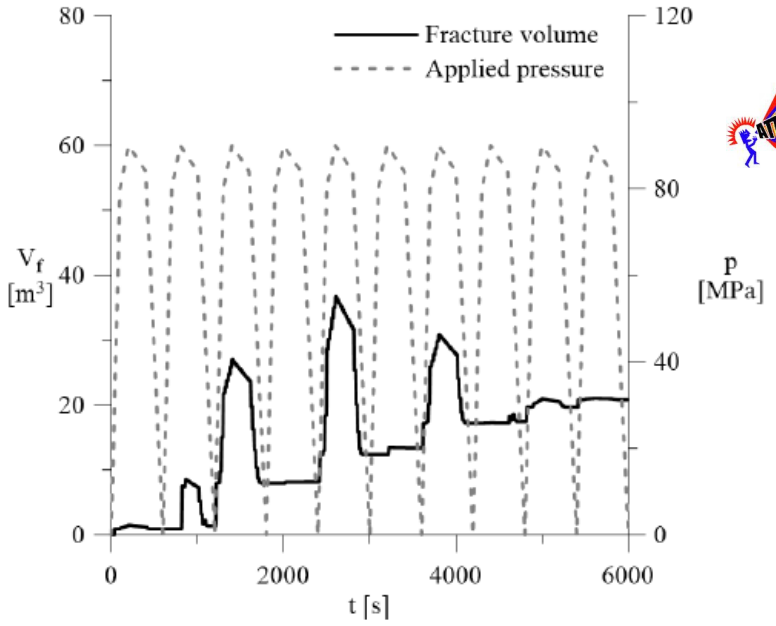

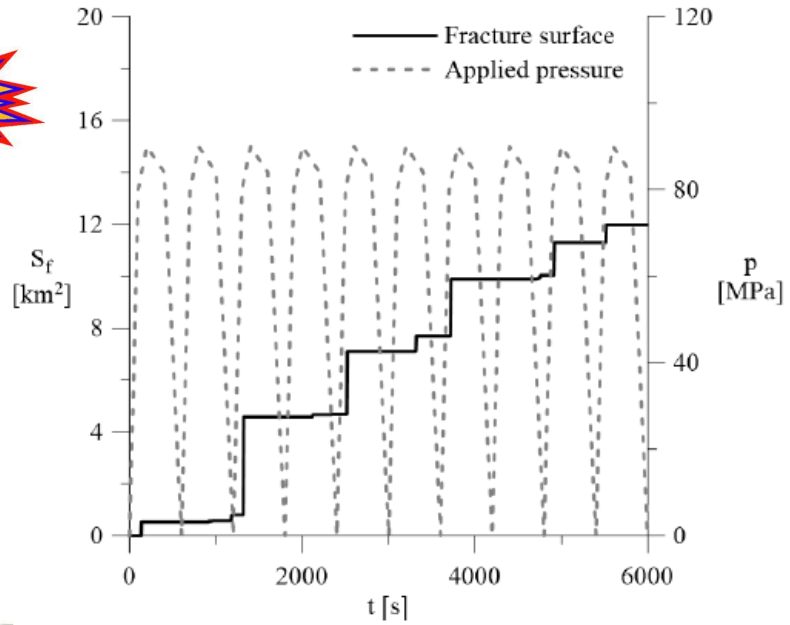

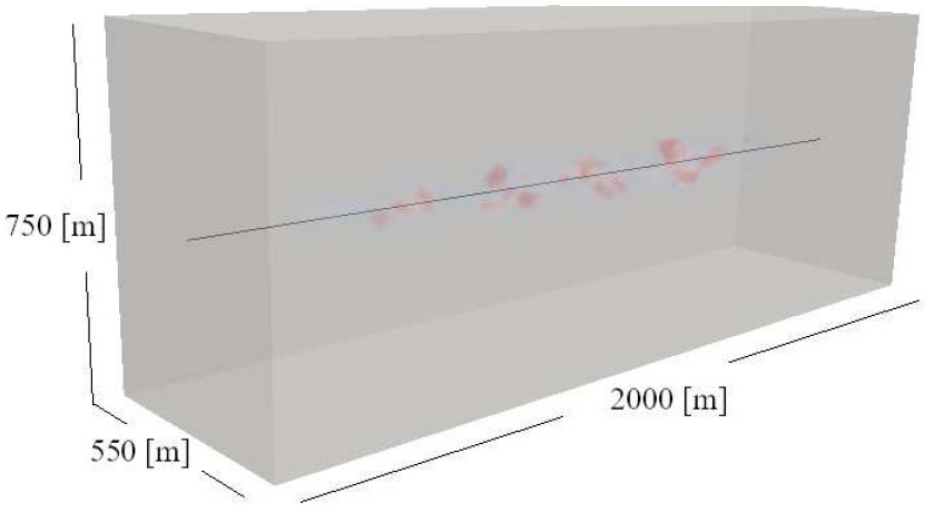

Michael Ortiz
IWS 12/08/20

Example: 3 boreholes, 45 injections

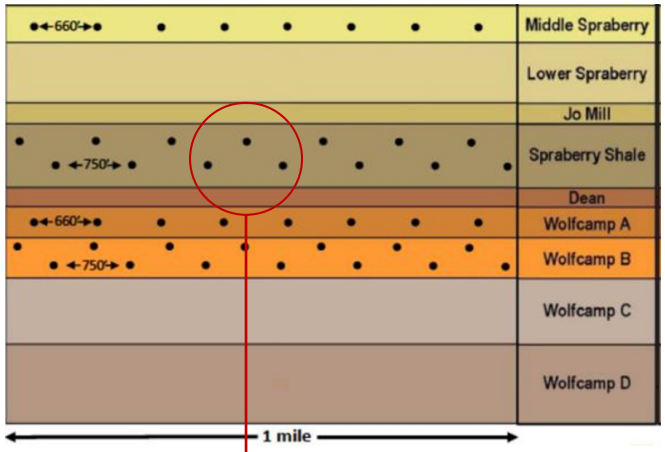

- End-on view of '*wine rack*' multi-bench, multi-well and multi-frac development (courtesy Apache)
- *Challenge*: Characterize *interaction* between boreholes, combined behavior, overall performance

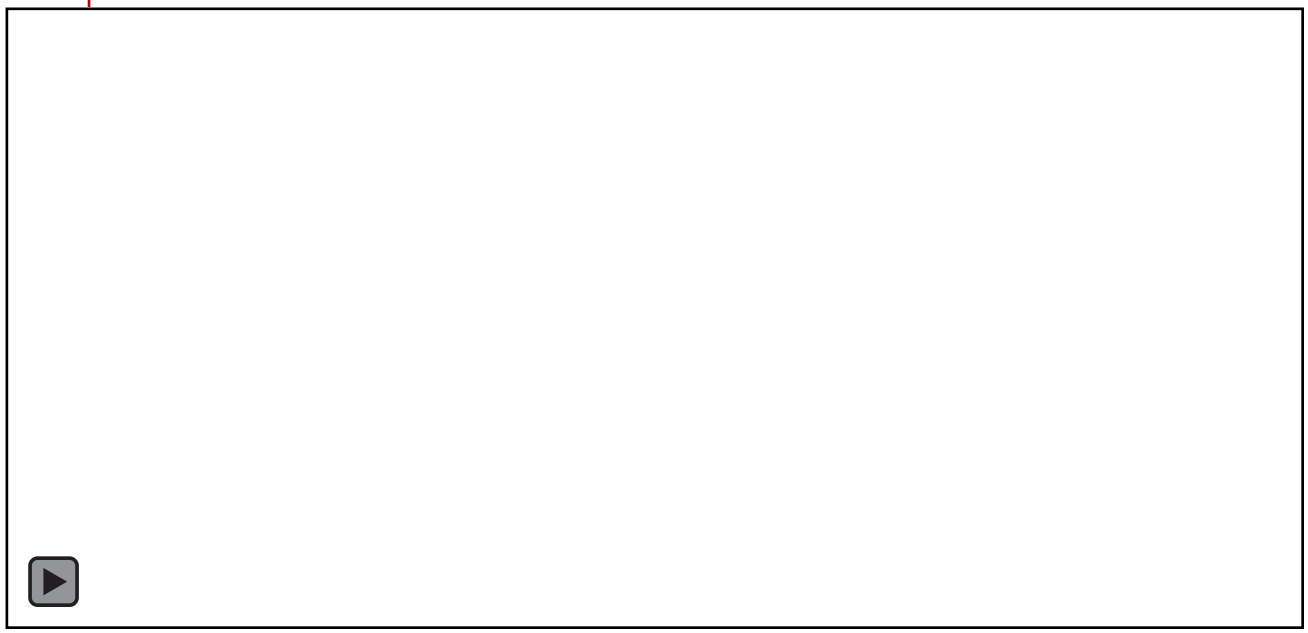

Michael Ortiz
IWS 12/08/20

Summary and outlook

Hydraulic Fracture (HF) is characterized by complex, mutiscale, multiphysics behavior

subgrid model

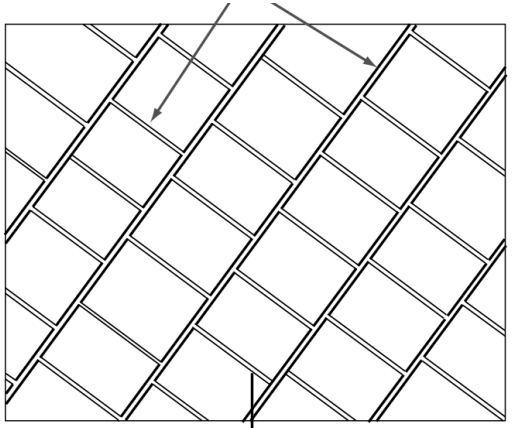

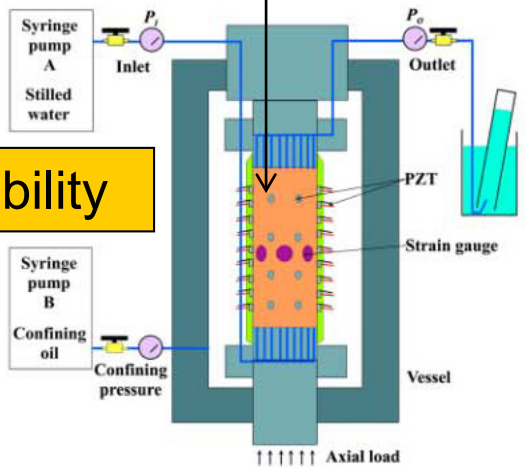

permeability

environmental impact analysis

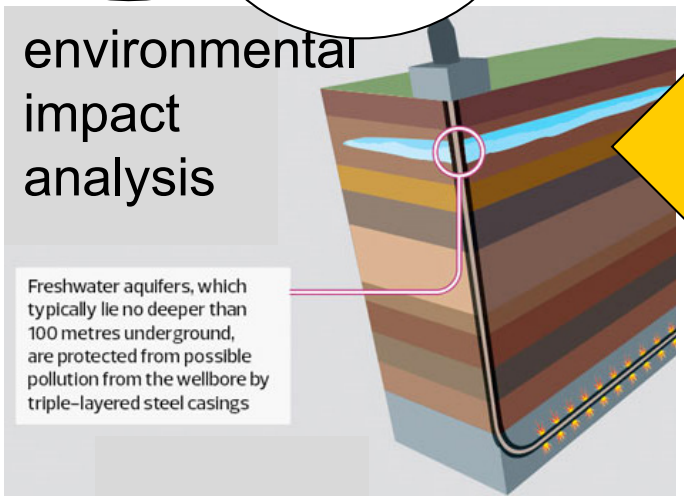

Lei et al., *Geophys. Res. Let.*, **38**, L24310, 2011

Michael Ortiz
IWS 12/08/20

Summary and outlook

subgrid model

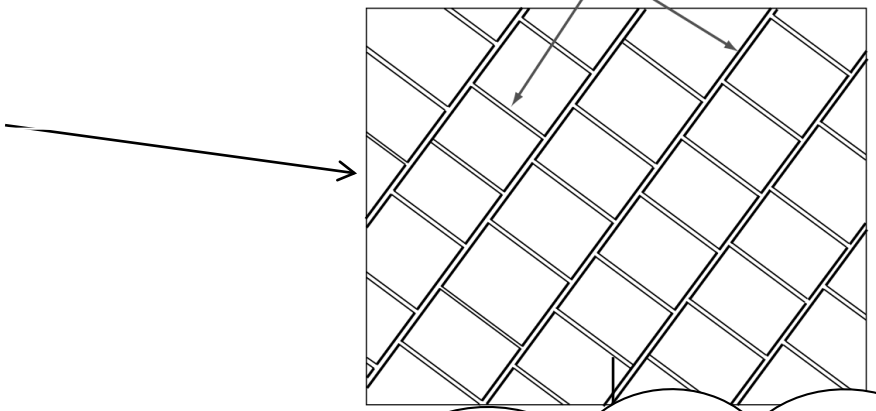

environmental impact analysis

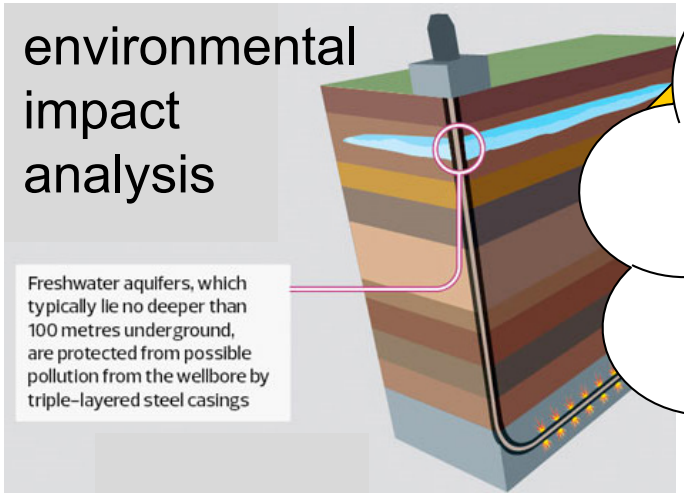

Permeability depends on fine structure of fracture patterns (no only averages)

38, L24

Summary and outlook

Sequential faulting is optimal at relaxing geostatic stresses

environmental impact analysis

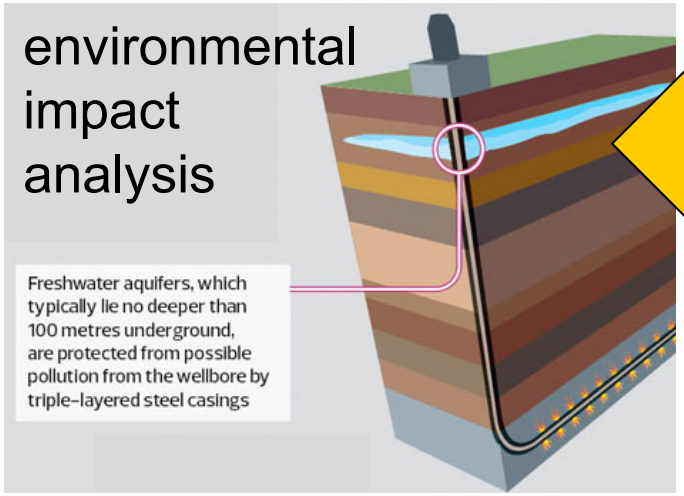

permeability

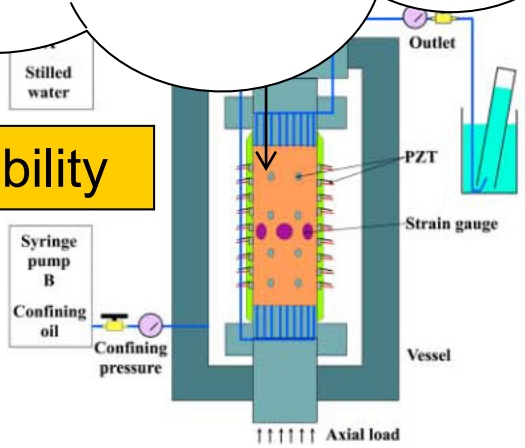

Lei et al., *Geophys. Res. Let.*, **38**, L24310, 2011

Summary and outlook

subgrid model

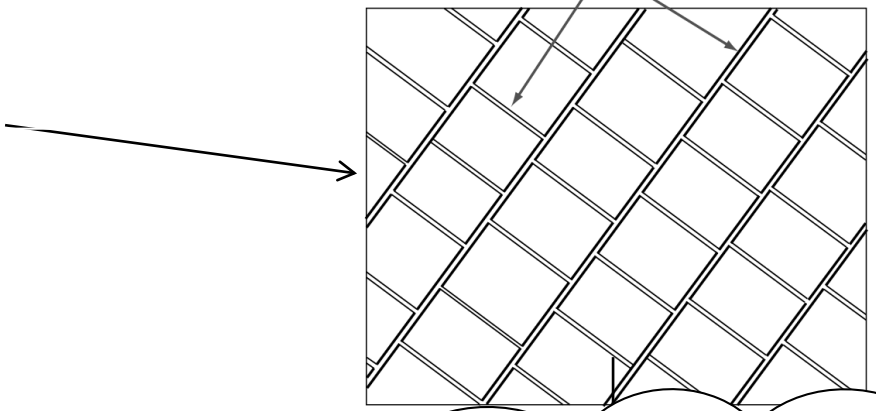

environmental impact analysis

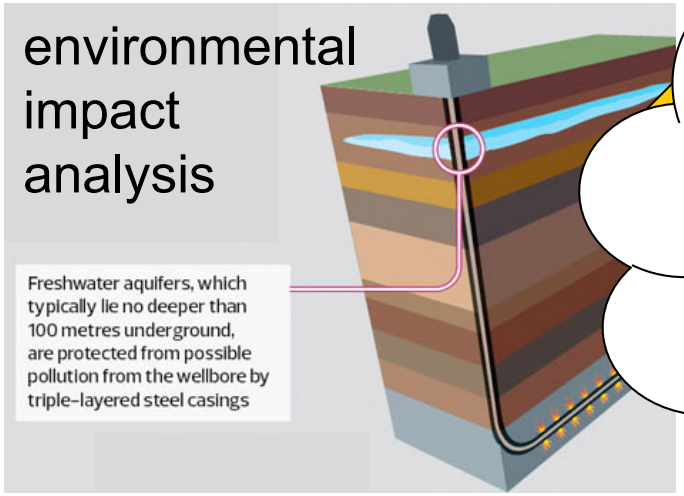

Sequential faulting introduces channels for fluid flow, resulting in enhanced permeability

38, L24

Summary and outlook

subgrid model

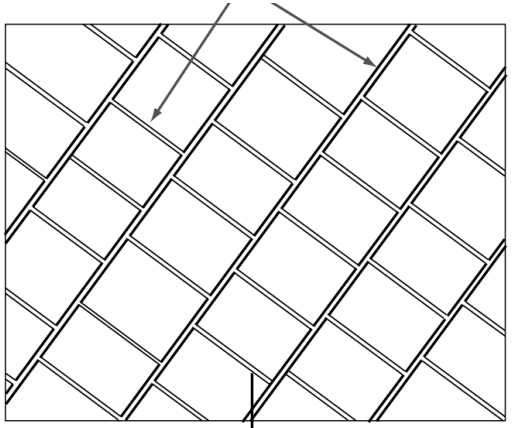

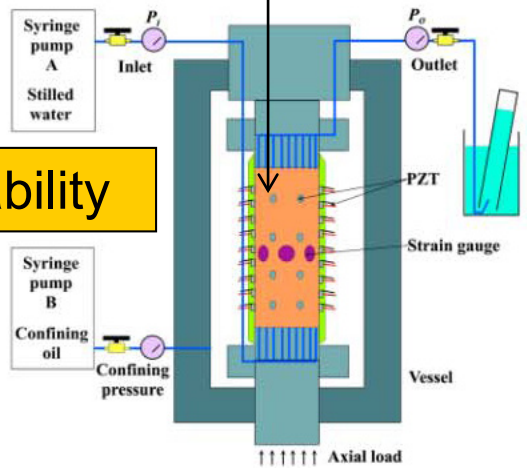

Potential payoff: HF process optimization, environmental impact (microseismicity, waste fluid disposal…)

Lei et al., *Geophys. Res. Let.*, **38**, L24310, 2011

Michael Ortiz
IWS 12/08/20